Study the Effect of Current Source Gate Driver on Traction Inverter

Dissertation submitted to
Visvesvaraya National Institute of Technology, Nagpur
in partial fulfillment of requirements for the award of
the degree

Master of Technology
in
Power Electronics and Drives

by

Yashahshree Thombre (MT23PED008)

under the guidance of

Dr. Mrs. Madhuri A. Chaudhari Mr. Milind Dighrasker

Department of Electrical Engineering
Visvesvaraya National Institute of Technology
Nagpur 440 010 (India)

June 2025

Study the Effect of Current Source Gate Driver on Traction Inverter

Dissertation submitted to
Visvesvaraya National Institute of Technology, Nagpur
in partial fulfillment of requirements for the award of
the degree

Master of Technology
in
Power Electronics and Drives

by

Yashahshree Thombre (MT23PED008)

under the guidance of

Dr. Mrs. Madhuri A. Chaudhari Mr. Milind Dighrasker

Department of Electrical Engineering
Visvesvaraya National Institute of Technology
Nagpur 440 010 (India)

June 2025

© Visvesvaraya National Institute of Technology (VNIT) 2025

Department of Electrical Engineering
Visvesvaraya National Institute of Technology, Nagpur

Declaration

I, Yashahshree Thombre, hereby declare that this dissertation titled, **"Study the Effect of Current Source Gate Driver on Traction Inverter"** is carried out by me in the Department of Electrical Engineering at Visvesvaraya National Institute of Technology, Nagpur. This work is original and has not been submitted earlier whole or in part for the award of any degree/diploma at this or any other Institute or University.

Yashahshree Thombre
Date : 29/5/25

Certificate

This is to certify that the dissertation titled **"Study the Effect of Current Source Gate Driver on Traction Inverter"** submitted by **Yashahshree Thombre** in partial fulfillment of the requirements for the award of the degree of **Master of Technology in Power Electronics and Drives**, VNIT Nagpur. The work is comprehensive, complete and fit for evaluation.

Dr. Mrs. Madhuri A. Chaudhari
Supervisor, Professor
Department of Electrical Engineering
VNIT, Nagpur - 440 010

Mr. Milind Dighrasker
Co Supervisor, Senior Director - Applications
ONSEMI, Bangalore - 560 066

Dr. B. S. Umre
Head, Department of Electrical Engineering
VNIT, Nagpur - 440 010
Date : 29.05.2025

विभाग प्रमुख / Head
विद्युत अभियांत्रिकी / Electrical Engi. Dept.
वि.रा.प्रौ.सं. / VNIT, Nagpur.

Department of Electrical Engineering
Visvesvaraya National Institute of Technology, Nagpur

NON-PLAGIARISM CERTIFICATE

Certified that M.Tech dissertation titled "Study the Effect of Current Source Gate Driver on Traction Inverter" submitted by Yashahshree Thombre , Enrollment No. MT23PED008, ID No. 30830 has been checked for plagiarism using TURNITIN software, and overlap is found within prescribed limit. A summary of the report is given below:

ORIGINALITY REPORT

26%	20%	18%	9%
SIMILARITY INDEX	INTERNET SOURCES	PUBLICATIONS	STUDENT PAPERS

Signature :
Name : Yashahshree Thombre
Enrollment No. : MT23PED008
Student ID : 30830
Date : 29/5/25

Dr. Mrs. Madhuri A. Chaudhari
Supervisor, Professor
Department of Electrical Engineering
VNIT, Nagpur - 440 010

ACKNOWLEDGMENTS

In the submission of my dissertation, I would like to extend my gratitude and sincere thanks to my guide **Dr. Mrs. Madhuri A. Chaudhari**, Department of Electrical Engineering, VNIT, for her constant motivation and support during the course of my work in the last year. I truly appreciate and value her valuable guidance and encouragement from the beginning to the end of both my projects.

I would like to extend my gratitude to **Mr. Milind Dighrasker**, Sr. Director System Applications team, Onsemi, who was my guide during the course of my internship. It was an invaluable learning experience for me.

I express my special thanks to **Mr. Jeevan Thomas, Mr. Vishwas K., Mr. Subbiah Palaniappan** who provided guidance whenever needed and kept a research friendly environment. From them I have gained not only extensive knowledge, but also a careful research attitude.

I extend my heartfelt thanks to the project evaluation committee **Dr. Pradyumna Chaturvedi**, **Dr. Jawahar Bhukya** and **Dr. Narendra A. Babu** for their guidance and comments.

I am also thankful to **Prof. Bhimrao S. Umre**, Head of the Department, Electrical Engineering for his permission and encouragement accorded to carry out the projects.

I am also obliged to **Dr. Prem Lal Patel**, Director of Visvesvaraya National Institute of Technology, Nagpur who maintained a good academic and amicable research environment making our studies at VNIT, Nagpur benficial and delightful.

I am immensely grateful to my parents,**Dr. Shashikant B. Thombre**, **Mrs. Neelakshi S. Thombre**. Their unwavering support, understanding, and sacrifices have allowed me to complete my master's degree and pursue my academic goals.

I am also grateful to all teaching and non-teaching staff members of the department of Electrical Engineering for their help during the course of project work.

Signature : 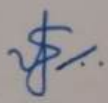
Name : Yashahshree Thombre
Enrollment No. : MT23PED008
Student ID : 30830

Abstract

The EVs are a increasingly becoming more popular mode of transport for the benefits they offer and the incentives that various governments provides. However, there is a significant impact on the power quality of the grid due to large-scale adoption of electric vehicles. MATLAB Simulink was used to analyse how increasing EV charging needs were causing power quality to deteriorate. The results were also verified using a real-time hardware simulator OPAL-RT. According to the study, the more EVs charging via the grid, the higher the Total Harmonic Distortion (THD). Further in order to maximise the efficiency of the EVs and lower the frequency of grid charging, a traction inverter is modelled using SiMetrix. A typical EV loading pattern is connected to the inverter for analysis.

As the power of traction inverters continues to rise, the demand for their efficiency and reliability becomes increasingly critical. Gate drivers are pivotal in determining the performance of these inverters. Traditionally, voltage source gate drivers (VSGDs) have been employed, but they come with inherent drawbacks. The external gate resistor in VSGDs contributes to higher losses and prolonged switching times. These issues are exacerbated at higher frequencies, leading to significant losses in the switches. Consequently, minimizing these losses is essential to enhance the overall efficiency of traction inverters.

To tackle these challenges, current source gate drivers (CSGDs) have been proposed as a superior alternative. Unlike VSGDs, CSGDs eliminate the need for an external resistor, providing a constant gate current during switching transitions. This results in reduced losses and faster switching times. The reduction in losses directly translates to improved efficiency of the traction inverter, which in turn shortens the charging cycle and extends the driving range of electric vehicles. By adopting CSGDs, the performance and reliability of traction inverters can be significantly enhanced, supporting the advancement of electric vehicle technology.

Keywords: G2V Charging, traction inverters, gate drivers

List of Figures

1.1 Electric car registrations and sales share in China, United States and Europe, 2018-2023, IEA 2024 . . . 2
1.2 Block diagram of Traction Inverter . . . 3
1.3 Voltage source gate driver . . . 5
1.4 Current source gate driver . . . 5
1.5 During turn ON . . . 5
1.6 During turn OFF . . . 5

2.1 Block diagram of EV . . . 13

3.1 Circuit Diagram of Charger box . . . 19
3.2 Simulation model of Charger box . . . 20
3.3 FFT of Grid Current . . . 21
3.4 FFT of Charging Current . . . 21
3.5 OPAL RT Waveform of Grid Current . . . 22
3.6 OPAL RT FFT of Grid Current . . . 22
3.7 OPAL RT Waveform of Charging Current . . . 23
3.8 OPAL RT Charging Current FFT . . . 23

4.1 N-Channel MOSFET Symbol . . . 26
4.2 MOSFET Turn ON Characteristics . . . 27
4.3 MOSFET Turn OFF Characteristics . . . 28
4.4 Power loss in MOSFET . . . 29
4.5 Double Pulse Test Circuit Diagram . . . 31
4.6 Results of the Double Pulse Test . . . 33
4.7 Switching Energy Loss . . . 34

5.1 WLTC Class 3b Drive Cycle . . . 36
5.2 Procedure to estimate the current profile . . . 37
5.3 Forces acting on the moving vehicle . . . 38
5.4 Traction Torque vs Time . . . 39
5.5 Current vs Time . . . 40
5.6 Power vs Time . . . 40
5.7 Typical Capacitance vs Drain-Source Voltage (Vds) . . . 43
5.8 Vds fall time . . . 43
5.9 Vds Rise time . . . 44
5.10 Rise time of Id . . . 45
5.11 Fall time of Id . . . 45
5.12 Switching energy loss during turning ON . . . 52
5.13 Switching energy loss during turning OFF . . . 52

6.1 Simulation model: Double Pulse Test using Voltage Source Driver . . . 53
6.2 Results for Voltage Source Double Pulse Test . . . 54

6.3 Simulation model: Double Pulse Test using Current Source Driver 54
6.4 Results for Current Source Double Pulse Test 55
6.5 Switching Energy during turning ON with respect to drain current 55
6.6 Switching Energy during turning OFF with respect to drain current 56
6.7 Simulation model of Three phase inverter 56
6.8 Inverter Output with Voltage source driver 57
6.9 Energy loss in inverter switch with Voltage Source Driver 57
6.10 Inverter Output with Current Source Driver 58
6.11 Energy loss in inverter switch with Current Source Driver 58
6.12 Hardware Setup of Double Pulse Test with Voltage Source Driver 59
6.13 DPT Evaluation Board 59
6.14 Waveforms observed on the oscilloscope: gate-source voltage (V_{gs}), drain-source voltage (V_{ds}), and the inductor current (I_L) 59

List of Tables

3.1 Grid Parameters and Load Values 20
3.2 Battery Parameters and Values 20
3.3 Rectifier Parameters and Their Values 20
3.4 DC/DC Converter Parameters 20

5.1 Values considered 41
5.2 Calculation of Various Forces 42
5.3 Switching Parameters and Energy Calculations when Vgs is applied . . . 49
5.4 Switching Parameters and Energy Calculations when ig is applied 51

6.1 Switching Energy for $I_g = 3A$ 55
6.2 Switching Energy for $V_{gs} = 15V$ 55

Symbols

C_{gs}	Gate-Source Capacitance
C_{gd}	Gate-Drain Capacitance
C_{ds}	Drain-Source Capacitance
C_{iss}	Input Capacitance
C_{oss}	Output Capacitance
C_{rss}	Reverse Recovery Capacitance
V_{gs}	Gate-Source Voltage
V_{gd}	Gate-Drain Voltage
V_{ds}	Drain-Source Voltage
I_d	Drain Current
V_{pl}	Miller Plateau Voltage
V_{th}	Gate Threshold Voltage
THD	Total Harmonic Distortion

List of Publications

1. Y. Thombre and M. Chaudhari, ”Study the effect of Current source gate driver on the performance of traction inverter,” 2025 Fourth International Conference on Smart Technologies for Power, Energy and Control (STPEC 2025), Goa, India, 2025. *(Submitted)*

Contents

Abstract i

List of Figures ii

List of Tables iv

Symbols v

1 INTRODUCTION 1
- 1.1 Background of Research . . . 1
- 1.2 Traction Inverters . . . 3
  - 1.2.1 Gate Drivers in Traction Inverters . . . 4
- 1.3 Research Gaps . . . 6
- 1.4 Research Objectives . . . 7
- 1.5 Contributions to the Research . . . 8
- 1.6 Thesis organization . . . 9

2 LITERATURE SURVEY 10
- 2.1 Introduction . . . 10
- 2.2 Impact of G2V . . . 11
- 2.3 Gate Drivers . . . 13

3 IMPACT OF EV CHARGING ON GRID 16
- 3.1 Introduction . . . 16
  - 3.1.1 Introduction of Harmonics in to the grid . . . 16
  - 3.1.2 Impact of G2V on the Grid . . . 18
- 3.2 Conclusion . . . 23

4 SWITCHING CHARACTERISTICS OF THE MOSFET AND DOUBLE PULSE TEST 25
- 4.1 Introduction . . . 25
- 4.2 Switching Characteristics of MOSFET . . . 25
  - 4.2.1 Overview of Power loss in MOSFET . . . 28
- 4.3 Double Pulse Test . . . 31
- 4.4 Conclusion . . . 34

5 CURRENT ESTIMATION AND SWITCHING TIME ANALYSIS 35
5.1 Introduction . . . 35
5.2 Vehicle dynamics . . . 35
5.2.1 Current Profile Estimation . . . 36
5.2.1.1 Sample Calculation . . . 41
5.2.2 Rise time and Fall time Calculation . . . 42
5.2.2.1 When Vgs is applied . . . 42
5.2.2.2 When ig is applied . . . 46
5.2.3 Sample Calculation . . . 46
5.3 Conclusion . . . 52

6 SIMULATION RESULTS AND ANALYSIS 53
6.1 Simulation of Double Pulse Test . . . 53
6.1.1 With Voltage Source Driver . . . 53
6.1.2 With Current Source driver . . . 54
6.1.3 Comparison of Switching Energy loss . . . 55
6.2 Simulation of Traction Inverter . . . 56
6.3 Hardware Setup of Voltage Source Driver Double Pulse Test . . . 58

7 CONCLUSION AND FURTHER SCOPE 60
7.1 Conclusion . . . 60
7.2 Future Scope . . . 60

Bibliography 62

CHAPTER 1

INTRODUCTION

1.1 Background of Research

Electric vehicles (EV) have become a more popular mode of transport over the past decade. Electric vehicles use electric motors powered by batteries instead of internal combustion engines (ICE). EVs offer the benefits of reduced greenhouse gas emissions and dependency on fossil fuels, low maintenance, thus being cost effective in the long run. The widespread adoption of EVs has been promoted by concerns over climate change, government incentives and advances in battery technology. As battery efficiency improves, EV are becoming more affordable, making them more appealing to the users. Many countries are emphasizing on the transition to electric mobility. Phasing out of ICE vehicles is one of the short term targets.

The electric vehicles now are available in all vehicle segments- from two-, three, four- wheelers to trucks and buses. The use of electric transport requires them to be charged through grid. Grid-to-Vehicle (G2V) is the conventional process where electric vehicles (EVs) draw power from the grid to charge their batteries. In contrast to Vehicle-to-Grid (V2G), where energy is sent from the vehicle back to the grid. The large-scale adoption of G2V presents challenges in terms of grid capacity and power quality, which must be managed to prevent negative impacts on the grid.

The electric power grid is the backbone of the modern electricity transmission and distribution network. From power plants to transmission lines to substations and distribution systems, the electricity supplied is uninterrupted and reliable. The grid balances the demand and supply of the electricity in the real-time. With the increasing population, industrialization and use of technology the demand for electricity is increasing. This poses a challenge to maintain stability and reliability of the grid.

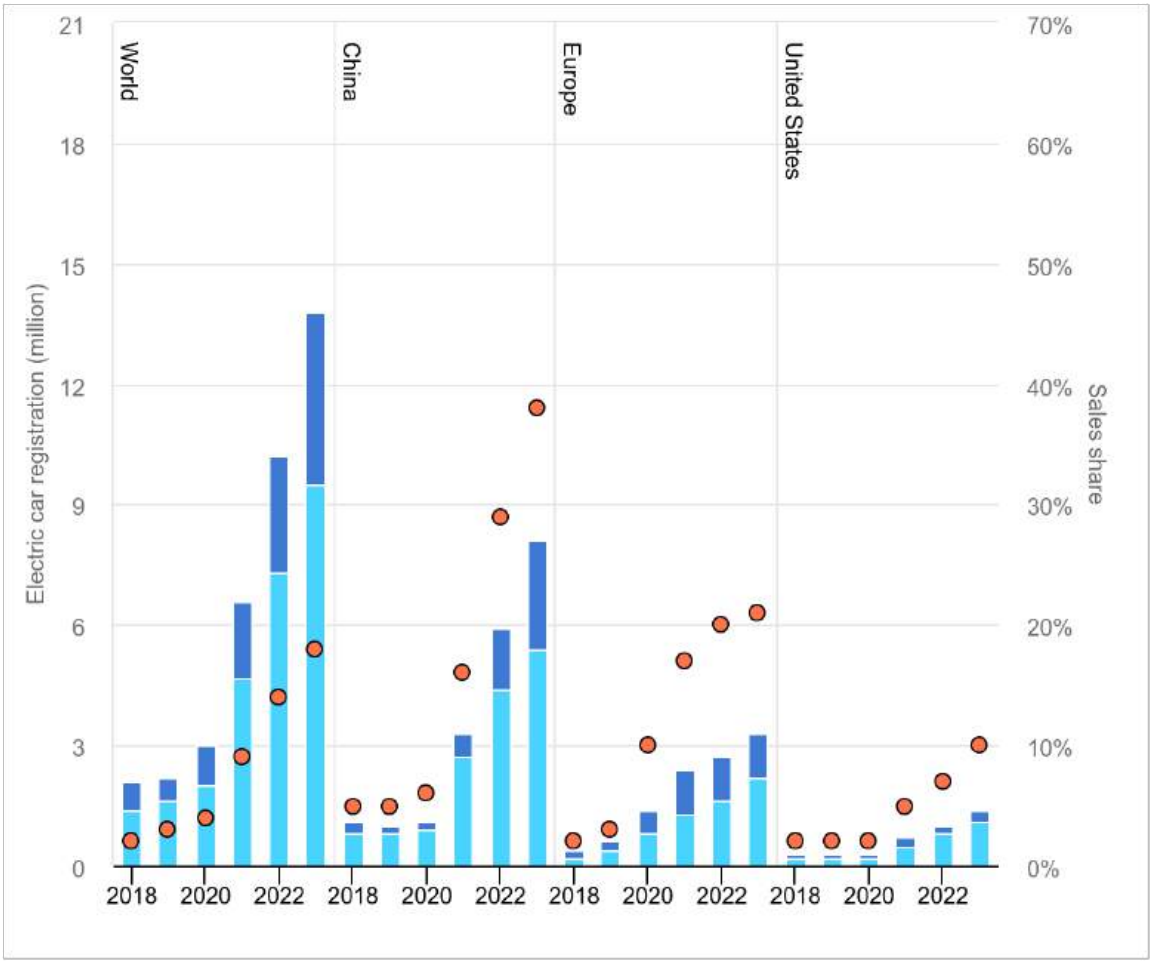

FIGURE 1.1: Electric car registrations and sales share in China, United States and Europe, 2018-2023, IEA 2024

EVs use power electronic devices such as rectifiers and inverters to convert alternating current (AC) from the grid to direct current (DC) to charge their batteries. These power electronic converters, if not properly designed or filtered, can introduce harmonics into the current drawn from the grid. When a significant number of vehicles are charging simultaneously, impact of EV charging on grid stability can be substantial. The harmonic currents generated by multiple EVs can degrade the quality of the power supplied by the grid, causing fluctuations in voltage and reducing the efficiency of energy distribution.

Figure 1.1 shows the trends reported by the IEA 2024 in Electric cars shows rapid increase in the consumption of Electric cars and indicated a robust growth and 40 million Electric cars on road by 2023 [1].

1.2 Traction Inverters

The proliferation of electric vehicles (EVs) has brought about significant changes in the way we consume and manage energy. As more vehicles rely on the grid for charging, the power quality of the grid profile has been increasingly compromised. One of the primary indicators of this deterioration is the rise in Total Harmonic Distortion (THD), which escalates with the growing number of EVs connected to the grid. Although the percentage of THD varies insignificantly across different types of grids, the overall impact on power quality remains a pressing concern.

A critical component in the operation of EVs is the traction inverter, which converts direct current (DC) from the battery into alternating current (AC) to power the electric motor. The efficiency and performance of these inverters are heavily influenced by the switches they employ, which are controlled by gate drivers. Among the various types of gate drivers, current source gate drivers have been identified as superior to voltage source gate drivers due to their numerous advantages.

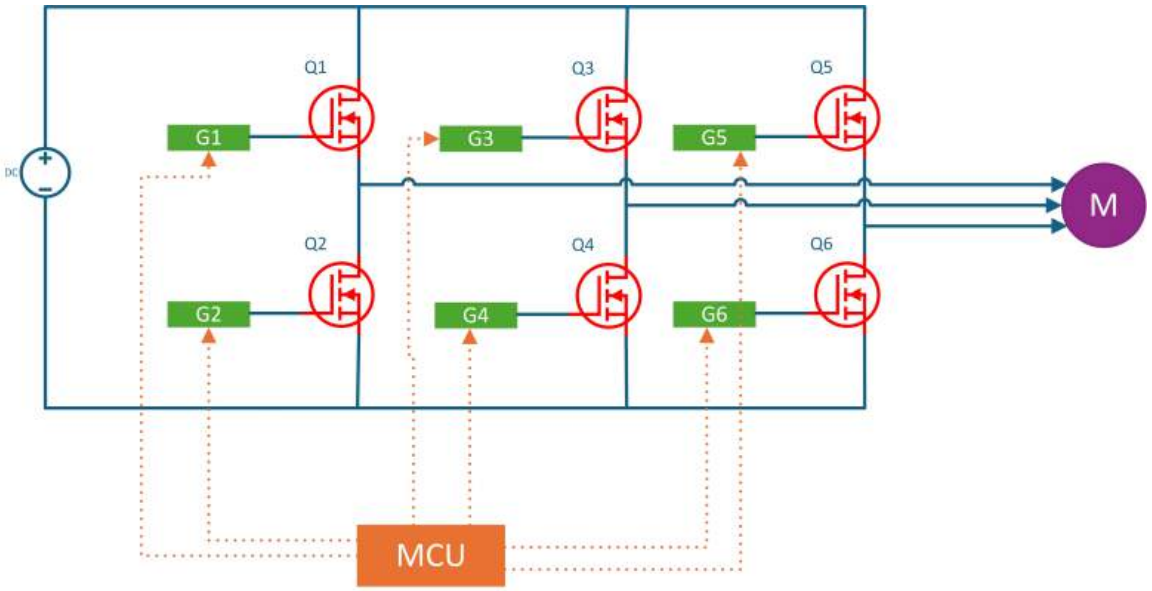

FIGURE 1.2: Block diagram of Traction Inverter

1.2.1 Gate Drivers in Traction Inverters

One of the key benefits of current source gate drivers is their ability to reduce switching losses in MOSFET switches. Switching losses occur when the MOSFET transitions between its on and off states, and minimizing these losses is crucial for enhancing the overall efficiency of the inverter. The double pulse test, a standard method for evaluating the performance of MOSFET switches, has shown that current source gate drivers can significantly lower these losses.

Improving the efficiency of the traction inverter has a direct impact on the driving range of EVs. With reduced switching losses, the inverter operates more efficiently, allowing the vehicle to travel longer distances on a single charge. This increased driving range means that EVs require fewer charging cycles, which in turn reduces the frequency of grid connections.

The reduction in charging cycles has a beneficial effect on the power quality of the grid. Each time an EV is connected to the grid for charging, power electronic devices within the vehicle inject harmonics into the grid voltage and current. These harmonics contribute to the overall THD, degrading the power quality. By decreasing the number of times EVs need to be charged, the injection of harmonics is minimized, leading to a more stable and cleaner power supply.

Maintaining good power quality is essential for the reliable operation of the grid and the devices connected to it. High levels of THD can cause malfunctions in sensitive equipment, increase losses in electrical systems, and lead to inefficient energy usage. Therefore, strategies that reduce THD, such as the adoption of current source gate drivers in traction inverters, are crucial for sustaining the integrity of the power grid.

As a result, the integration of current source gate drivers in EV traction inverters presents a promising solution to the challenges posed by increased grid charging. By enhancing inverter efficiency and extending driving range, these gate drivers contribute to fewer charging cycles and reduced harmonic injections. This approach not only supports

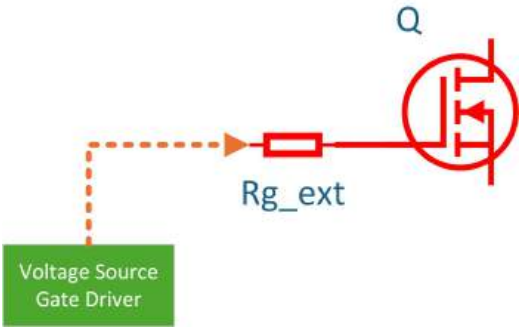

FIGURE 1.3: Voltage source gate driver

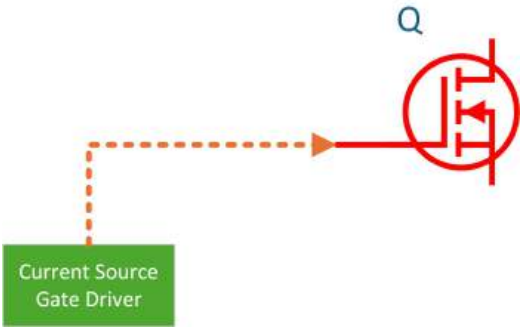

FIGURE 1.4: Current source gate driver

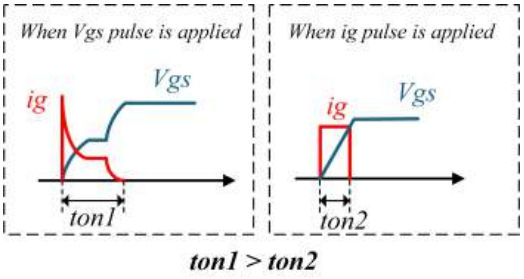

FIGURE 1.5: During turn ON

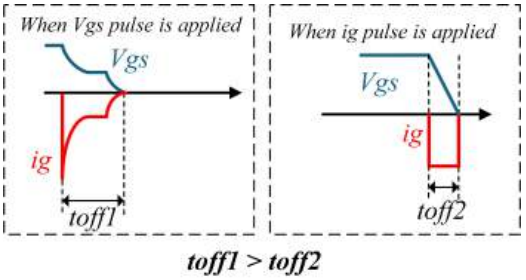

FIGURE 1.6: During turn OFF

the growth of the EV market but also ensures the maintenance of high-power quality in the grid, benefiting both consumers and the broader energy infrastructure.

EVs use power electronic devices such as rectifiers and inverters to convert alternating current (AC) from the grid to direct current (DC) to charge their batteries. These power electronic converters, if not properly designed or filtered, can introduce harmonics into the current drawn from the grid. When a significant number of vehicles are charging simultaneously, impact of EV charging on grid stabiltiy can be substantial. The harmonic currents generated by multiple EVs can degrade the quality of the power supplied by the grid, causing fluctuations in voltage and reducing the efficiency of energy distribution.

Traction inverter are intergral part of the EV power train. The traction inverters converts the DC from the battery to AC for the electric motor. The inverter output controls the speed and torque of the motor. The efficiency has a direct impact on the power dissipation and reliabilIty.

Increasing the efficiency of the inverter can reduce charging cycle of the EV. Consequently, the EV will be connected to the grid lesser no. of times and thus a good

power quality of the grid can be maintained. In addition, it will also increase the driving range of the vehicle.

A current source gate driver is proposed to reduce losses in the inverter switches and increase their efficiency. The benefits of current controlled gate drivers are that they provide faster turn ON and turn OFF thereby reducing the switching losses, operations at higher frequencies, removal of external resistors, etc. As per a report by Texas Instruments, a real-time control MCU, a variable gate driver and a bias supply are three key components to boost the efficiency of the traction inverters.

1.3 Research Gaps

The research gaps associated with the study are

1. **Limited Exposure to Real-Time Simulation of EV Charging Through Grid**
   This involves the need for more practical, real-time simulations of electric vehicle (EV) charging processes connected to the power grid. Such simulations can help estimate the impact of EV charging on the power quality of the grid, including aspects like voltage stability, frequency regulation, and overall grid reliability.

2. **Use of Current Source Gate Drivers to Improve Traction Inverter Performance for High Voltage Applications**
   This point highlights the potential benefits of using current source gate drivers in traction inverters, especially for high voltage applications. Current source gate drivers can enhance the performance of traction inverters by providing better control, efficiency, and reliability, which is crucial for the demanding conditions of high voltage operations.

3. **Limited Research on Current Source Gate Drivers**
   This acknowledges that there is a scarcity of research and studies focused on current source gate drivers. More research is needed to fully understand their capabilities,

advantages, and potential applications in various fields, including EV technology.

4. **Mathematical Analysis of Power Loss in SiC Switches**
   This involves conducting a detailed mathematical analysis to compare power loss in silicon carbide (SiC) switches when driven by voltage source gate drivers versus current source gate drivers. The analysis aims to quantify the differences in efficiency and performance between the two types of gate drivers.

5. **Determination of the Driving Range Increase of the EV**
   This point focuses on evaluating how the use of current source gate drivers can potentially increase the driving range of an electric vehicle. By improving the efficiency and performance of the traction inverter, current source gate drivers may contribute to extending the distance an EV can travel on a single charge.

1.4 Research Objectives

Electric vehicles (EVs) can decrease the quality of power in the grid. Limited research has been conducted on EV components to reduce the frequency of charging via the grid, which consequently reduces the Total Harmonic Distortion (THD) injected into the grid profile. The objective of this research is to provide an alternative to the conventional voltage source gate driver. This study analyzes the advantages of the current source gate driver over the voltage source gate driver.
Following are the objectives of the research:

- **Study the impact of EV charging on the grid:** EV charging can increase peak demand, cause localized grid overloads, and require significant infrastructure investment

- **Estimating the power loss in MOSFET:** Determining the power loss in the MOSFET is essential to understand where the losses are taking place.
- **Advantages of Current source Gate Drivers over Voltage source gate drivers:** Gate drivers have a direct impact on the switch performance.
- **Simulating the Double Pulse Test:** Simulation to identify the losses incurred in the

1.5 Contributions to the Research

- **EV Charger Simulation:** A EV charger has been simulated using MATLAB Simulink and a analysis of the THD of Grid voltage and current has been carried out.
- **Study of advantages of Current Source Gate Driver:** The benefits of Current Source Gate Drivers over the voltage source gate driver has been studied.
- **Analysis and calculation of Power loss in MOSFET:** Based on the switching characteristics of the MOSFET, the Conduction and Switching Power losses incurred during the charging of the gate are calculated using the gate charge and gate-source voltage.
- **Current profile estimation:**A current profile has been derived from a standard speed profile a vehicle. This current is the inverter output current which is equal to the drain current of the MOSFET.
- **Simulation Setup:** Created a circuit design in a Simetrix model, incorporating the MOSFET and configuring the double pulse test parameters on a MOSFET Module to evaluate switching performance, including switching losses to understand the MOSFET's behavior is developed.

1.6 Thesis organization

. This thesis focuses on the analysis power quality issues introduced due to the increasing EV charging through grid and study the performance of an traction inverter when using a current source driver and using voltage source driver. This is thesis organized as follows:

- **Chapter 1** contains a detailed introduction to the interconnection of the grid and electric vehicles and traction inverters.
- **Chapter 2** contains literature survey regarding impact of EVs on grid and modeling of traction inverters .
- **Chapter 3: Impact of EV Charging on Grid** contains simulation of EV charger for G2V mode of operation and analysis of THD due to increasing EV penetration.
- **Chapter 4: Switching characteristics of the MOSFET and Double Pulse Test** contains a detailed explanation of the turning on and turning off of the MOSFET and importance of the Double Pulse Test process.
- **Chapter 5 Current Estimation and Switching Time Analysis** discusses a preliminary procedure to derive a current profile from a standard drive cycle.
- **Chapter 6: Simulation Results and Analysis** contains Simetrix simulation of the traction inverter and the double pulse test using voltage driver and current driver is presented here.
- **Chapter 7:** This chapter gives conclusion and future scope

CHAPTER 2

LITERATURE SURVEY

2.1 Introduction

The rapid adoption of electric vehicles (EVs) has brought significant advancements in sustainable transportation, but it has also introduced new challenges to the electrical grid. The integration of electric vehicles (EVs) into the power grid presents several challenges. Voltage and current distortions due to harmonics can degrade power quality, while the increased load on distribution transformers and feeders can strain these components, potentially reducing their lifespan. Additionally, thermal heating of grid equipment can further impact performance and durability. Beyond these issues, peak demand spikes from simultaneous EV charging can stress the grid, necessitating infrastructure upgrades. The unpredictable nature of EV charging poses challenges to grid stability and balancing supply and demand. Furthermore, the increased connectivity of EV charging stations introduces cybersecurity risks, and efficient energy storage solutions are needed to manage variable loads and ensure a stable power supply. One of the most pressing concerns is the degradation of power quality, particularly the increase in Total Harmonic Distortion (THD). As EV charging stations proliferate, especially in urban and residential areas, the non-linear nature of power electronics used in chargers contributes to harmonic injection into the grid. This elevated THD can lead to overheating of transformers, increased losses, and malfunctioning of sensitive equipment, thereby necessitating robust mitigation strategies.

In this context, traction inverters—key components in EV powertrains—play a pivotal role in determining the overall electromagnetic compatibility and efficiency of the vehicle. These inverters are responsible for converting DC power from the battery into AC power for the motor, and their switching behavior significantly influences the harmonic profile of the system. Traditional voltage source gate drivers, while widely used, often struggle to

maintain optimal switching performance under varying load and temperature conditions, which can exacerbate harmonic emissions and reduce system reliability.

Current source gate drivers have emerged as a promising alternative, offering precise control over gate charge dynamics and enabling consistent switching behavior across a wide range of operating conditions. By regulating the gate current directly, these drivers can achieve linear voltage transitions, reduce switching losses, and minimize electromagnetic interference (EMI). This level of control is particularly beneficial in traction inverters, where high-speed and high-efficiency switching is critical for both performance and compliance with grid standards.

This literature survey aims to explore the growing body of research addressing the impact of EV charging on grid THD and the technological advancements in gate driver design for traction inverters. Special emphasis is placed on the role of current source gate drivers in enhancing inverter performance, reducing harmonic distortion, and supporting the broader goal of integrating EVs into the power grid without compromising stability or efficiency.

2.2 Impact of G2V

The integration of electric vehicles (EVs) into the power grid introduces harmonics, which distort voltage and current profiles. These distortions can degrade power quality, increase losses in electrical components, and cause thermal stress on grid equipment. Understanding the impact of harmonics is crucial for developing strategies to maintain grid stability and performance.

Higher penetrations of electric vehicles (EVs) significantly impact both line and generator loading. In a scenario with a 3.3kW load, the maximum line load at 1 % EV penetration is 34.7 %. This increases to 53.42 % at 25 % penetration and further to 75.75 % at 50 % penetration, demonstrating the substantial strain on the power grid. Similarly, the highest loaded generator at 1 % penetration is at 64.03 %. This rises to 89.3 % at 25 % penetration and exceeds the operating limit at 50 % penetration, reaching 126.17 %.

These figures illustrate how the growing demand from EVs can significantly stress the grid infrastructure [2]. The study presents a comprehensive assessment of the impact of plug-in electric vehicle (PEV) penetration on distribution network investments and energy losses. It analyzes two large-scale distribution areas—urban and rural—across three PEV penetration scenarios (35 %, 51 %, and 62 %). Results indicate that peak-hour charging can lead to network reinforcement costs up to 19 % of current infrastructure costs, with urban areas being more affected. Smart charging strategies could reduce these costs by 60–70 %, and shifting charging to off-peak hours could yield an additional 5–35 % reduction. Energy losses may increase by up to 40 % during off-peak hours under high PEV penetration. [3]. A study evaluates the performance of 21 distribution grids across Austria, Germany, and the Netherlands under four electric vehicle (EV) penetration levels (0%, 20%, 50%, 80%) and two seasonal conditions (winter and summer). It highlights that uncontrolled EV charging significantly contributes to peak load congestion, especially in suburban grids due to higher household and vehicle densities. While German grids showed resilience due to higher design redundancy, Austrian grids experienced the most congestion, including voltage drops even at moderate EV levels. Dutch grids faced transformer overloading, influenced by both grid characteristics and EV charger availability. Despite 13 grids showing no congestion even at 80% EV penetration, a few grids exhibited severe issues, suggesting the need for smart charging strategies and targeted infrastructure upgrades [4]. The effect of different % EV penetration on Loss-Of-Life of Distribution Transformers was presented in this paper. Single day energy requirements of EVs at home on single DT based on SOC of battery was investigated before calculating the LOL of DT. The home arrival time and the mileage driven were sampled to determine the EVs daily charging profile. The Monte Carlo technique was used to generate data required for EVs charging demand. The percentage EVs considered to charge were 20%, 40%, 60%, 80% and 100% of the number of consumers connected to DT. EV charging demand causes substantial DT overloading when most of EVs are charged at the same time. It is therefore suggested that the peak load or overload on DT can be avoided by charging the EVs at different time [5]. Another paper examines the impact of uncontrolled EV charging on two distribution grids in the Netherlands. The results show that higher EV penetration increases transformer and line overloading, and

node under-voltage, especially in sub-urban grids [6]. Using data driven approach, Monte-Carlo analysis based simulations on aggregate model of 100 EV charging events were conducted. The result shows the distribution of EV charger type plays a significant role in this process that a higher ratio of public and semi-public charger could drastically improve the excessive PV decreasing procedure. Specifically, the median of excess PV energy reduces by almost 50% from 0.4 to 0.2 MWh on a given day when home charger ratio is declined from 70% to 25% within this 100 charging events. Furthermore, none of the grids experience overloads or under-voltage issues with the introduction of EVs even without any presence of any PV. It can be inferred from this that all three simulated grids can manage EV penetration beyond the maximum level set in this research work. If closely looked at the rural and urban grids, it is seen that the grids were operating at low loading values to begin with. Hence, in order to make them function near its technical limits, would mean addition of very large loads. The number of EVs to make such an impact would be very significant. Hence the overloading was absent in each of the grids. All the grid are oversized, robust and operationally efficient with the given simulation conditions[7]. Large deployment of EVs and PHEVs is expected to lead to potential problems for existing power networks.Subsequently resulting in violation of supply/demand matching and statutory voltage limits. Under certain operating conditions, they may also lead to power quality problems and voltage imbalance. The latter is unlikely to exceed the statutory limit if EVs are reasonably distributed among the three phases [8].

2.3 Gate Drivers

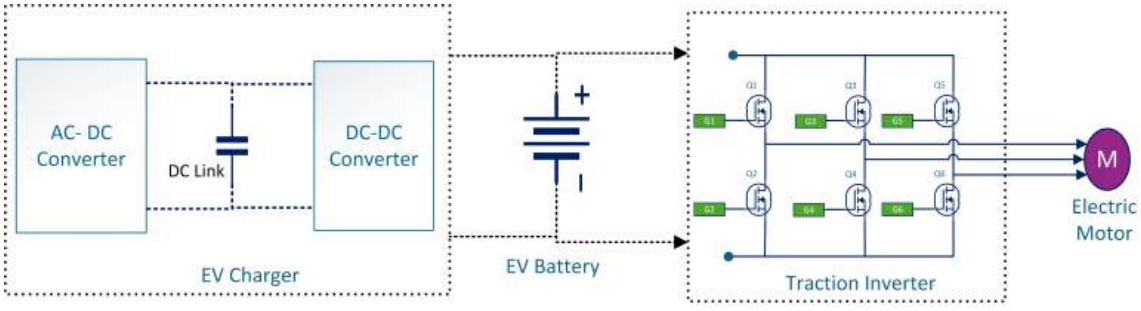

FIGURE 2.1: Block diagram of EV

Figure 2.1 shows the block diagram of an EV architecture.The EV charger circuit includes an AC-DC converter that transforms AC from the grid into DC, a DC link capacitor, and a DC-DC converter that adjusts the voltage according to the battery's requirements. The battery is connected to a traction inverter, which powers the electric motor or engine of the vehicle. A gate driver is used to drive the switches in the power electronics converters, and directly impacts the performance of the inverter.

Electric vehicle (EV) designs must balance efficiency, cost, and sustainability.

Traction inverters are essential components in modern power electronics, playing a significant role in enhancing the efficiency and environmental friendliness of automobiles. The paper provides a detailed analysis of various production traction inverter designs and highlights the adoption of Wide Bandgap (WBG) devices, particularly Silicon Carbide (SiC), which are beginning to see widespread use, starting with Tesla's Model 3. These devices promise improved efficiency and power density, and their costs are expected to decline as demand increases. Additionally, active gate drive designs have shown up to a 30% reduction in IGBT turn-off losses, with fully integrated active gate drive ICs likely to become more common, reducing cost and complexity. The paper also discusses the benefits of tighter integration of the inverter with other vehicle electronics, which can lead to cost and weight savings, and further power density improvements [9].

A CSG feeding a constant gate current during the whole switching transient regardless of the influence by the large internal gate resistance in the SiC MOSFET was proposed. A double pulse test conducted between the conventional VSG and proposed CSG with shows that the switching loss of the proposed CSG is one third of the conventional VSG at full load [10]. The behavior and performance of both the current source driver (CSD) and the conventional voltage source driver (VSD) were analyzed under conditions involving non-zero initial inductor current. The comparative results indicate that the CSD offers superior performance, including faster switching, lower switching losses, and reduced conduction losses when compared to the VSD. Overall, the CSD achieves a 55 % reduction in total power loss relative to the VSD in [11]. Compared to voltage source drivers (VSDs), CSDs reduce switching times by up to 75 % during turn off and 50 % during turn on, making them well-suited for high-frequency, high-voltage, and series/parallel device applications [12].

A comparison made by another study between the conventional VSG and the proposed CSG with DPTs. The results show that the proposed CSG shortens the turn on and turn off times by 67 % and 50 %, respectively, at full-load condition.Furthermore, the switching loss reduction of 68 % is observed against the conventional VSG [13]. Furthermore, the proposed current source gate drive circuit for power MOSFETs achieves quick turn on and turn off transition times to reduce switching and conduction losses in power MOSFETS and can recover a portion of the CV2 gate energy normally dissipated in a conventional driver. The driver provides superior performance in comparison to conventional drivers. Experiment carried out on a boost converter at 1MHz, 5V input, 10V/5A output using the proposed driver achieves a 2.9 % efficiency improvement at 5V gate drive representing a loss savings of 24.8 % in comparison to a conventional driver [14].

CHAPTER 3

IMPACT OF EV CHARGING ON GRID

3.1 Introduction

The increasing penetration of electric vehicles (EVs) on the grid affects its power quality. The voltage and current profiles become distorted due to the introduction of harmonics. This additional load on distribution transformers and feeders can impact their performance and reduce their lifespan. Furthermore, these devices may experience thermal heating.

- The introduction of EVs leads to voltage and current profile distortions, primarily due to harmonics.
- The additional load from EV charging can strain distribution transformers and feeders, potentially reducing their lifespan and efficiency.
- Increased load can cause thermal heating of grid components, impacting their performance and durability.

This chapter discusses the impact of harmonics in detail.

3.1.1 Introduction of Harmonics in to the grid

The integration of electric vehicles (EVs) into the power grid is a significant step towards sustainable transportation. However, this transition brings several challenges that affect the grid's performance and reliability. Harmonics are a critical issue arising from the integration of EVs into the power grid. These are voltage or current waveforms that deviate from the fundamental frequency, typically caused by non-linear loads such as EV chargers. The presence of harmonics can lead to several adverse effects:

- **Voltage Distortion:** Harmonics can cause voltage distortions, leading to poor power quality and potential operational issues for sensitive equipment.
- **Increased Losses:** Harmonics increase the losses in electrical components, reducing the overall efficiency of the power system.
- **Thermal Stress:** The additional heat generated by harmonic currents can accelerate the aging of transformers and other grid equipment.
- **Resonance Issues:** Harmonics can cause resonance in the power system, leading to over voltages and potential damage to equipment.

Electric vehicles introduce harmonics into the grid primarily through their charging infrastructure. Most EV charging stations (EVSEs) use power electronics to convert AC from the grid into DC to charge the vehicle's battery. The conversion process typically involves rectifiers, which can draw current in a non-linear fashion, leading to harmonic distortion. For example, when the rectifier in the charging station draws current from the grid, it does so in a series of pulses rather than in a smooth sinusoidal waveform. These pulses, caused by the switching of power transistors in the rectifier, create harmonic currents at multiples of the grid frequency (e.g., 2nd, 3rd, 5th harmonics). These harmonics are then injected into the grid, causing the overall waveform to deviate from the ideal sinusoidal shape.

In addition, some EVs are equipped with onboard chargers that may have their own power conversion circuits, which can also contribute to harmonic distortion. If many EVs are charging in close proximity, the combined effects of these harmonic currents can accumulate, leading to significant distortion in the local power network.

The degree of harmonic distortion depends on several factors, such as the design of the EVSE, the type of rectifier used, the switching frequency of the power electronics, and the number of EVs charging at the same time. Older charging stations and less efficient power conversion designs are typically more prone to producing high levels of harmonics, although advancements in charging technology and filtering techniques are helping mitigate these effects.

Electric vehicles offer substantial environmental benefits, but their widespread adoption introduces new challenges for grid stability, particularly in terms of harmonic distortion. EVs, through their charging processes, generate harmonic currents that can distort the grid's sinusoidal waveform, affecting both the vehicles and the grid's infrastructure. Managing and mitigating the impact of these harmonics is essential to ensuring a reliable, efficient, and sustainable integration of EVs into the energy system. By improving charging technologies, using harmonic filters, and implementing smart charging strategies, the negative effects of harmonics on the grid can be reduced, allowing for a smoother transition to an electrified transportation system.

Grid-to-Vehicle (G2V) is the conventional process where electric vehicles (EVs) draw power from the grid to charge their batteries. In contrast to Vehicle-to-Grid (V2G), where energy is sent from the vehicle back to the grid, G2V involves only the charging phase where the grid supplies power to the EV, typically through charging stations. G2V is the most common mode of interaction between EVs and the grid today.

G2V is vital in the context of the energy transition as it allows for the widespread adoption of EVs, providing a cleaner alternative to traditional internal combustion engine vehicles. Charging EVs using grid power allows them to serve as an integral part of reducing overall emissions, especially when the grid is supplied by renewable energy sources. However, the large-scale adoption of G2V presents its own set of challenges, especially in terms of grid capacity and power quality, which must be managed to prevent negative impacts on the grid.

3.1.2 Impact of G2V on the Grid

The primary concern with G2V is its effect on the grid's load profile. As more EVs are deployed and their adoption increases, the demand for electricity, particularly during peak charging hours (such as evenings when people return home), could put additional strain on the grid. If too many vehicles are charged simultaneously without proper management, it can result in voltage fluctuations, overloads, and the need for additional generation and transmission capacity. Charging a large number of EVs could increase the peak demand

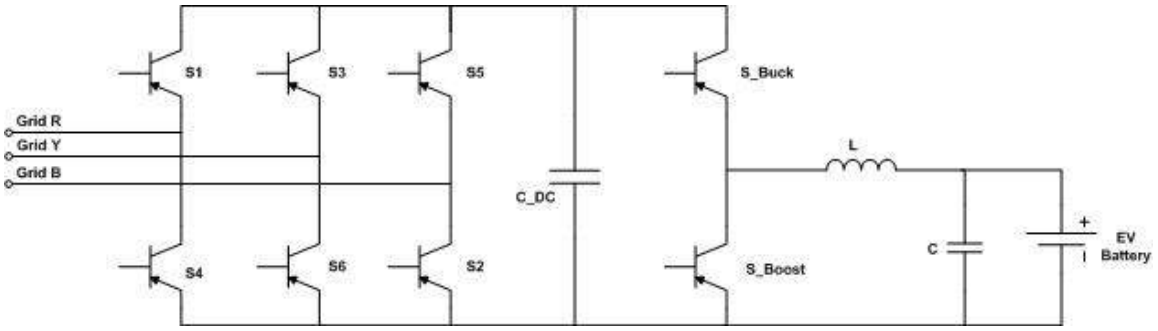

FIGURE 3.1: Circuit Diagram of Charger box

significantly, leading to higher electricity costs and, in some cases, the necessity for grid upgrades to accommodate this new demand.

From the perspective of grid stability, G2V poses challenges related to the timing and synchronization of charging loads. Without careful coordination, such as through smart charging systems, the grid could experience sudden spikes in demand, especially during peak hours, contributing to increased pressure on existing grid infrastructure. Smart charging solutions, which can schedule charging during off-peak hours or dynamically adjust charging rates based on grid conditions, can help alleviate these issues by spreading the load more evenly over time.

Another challenge is the potential impact on power quality due to harmonics generated by the charging process. Much like with V2G, the power electronics used in the charging process can generate harmonics, which may distort the waveform of the current drawn from the grid. However, this is generally less of a concern with G2V than with V2G, as the charging process typically involves less frequent switching compared to discharging.

MATLAB Simulation

A MATLAB simulation of an EV charger with the battery ratings given in Table 3.2 connected to the grid of rating as given in Table 3.1 has been performed. The circuit diagram 3.1 has been designed with parameters given in Table 3.4.

TABLE 3.1: Grid Parameters and Load Values

Grid Parameters	Values
VL-L RMS	415V
Load	3-Phase, 1kW

TABLE 3.2: Battery Parameters and Values

Battery Parameters	Values
Nominal Values	320V
Ah Rating	94.5 Ah
kWh Rating	30.2 kW
%SOC	60%

TABLE 3.3: Rectifier Parameters and Their Values

Rectifier Parameters	Values
VL-L RMS	415 V
DC Link Voltage	700 V
DC Link Capacitance	0.21 mF

TABLE 3.4: DC/DC Converter Parameters

DC/DC Conv. Parameters	Values
Output Voltage	350V
Inductor	390 mH
Capacitor	0.27 µF
Duty ratio	0.5

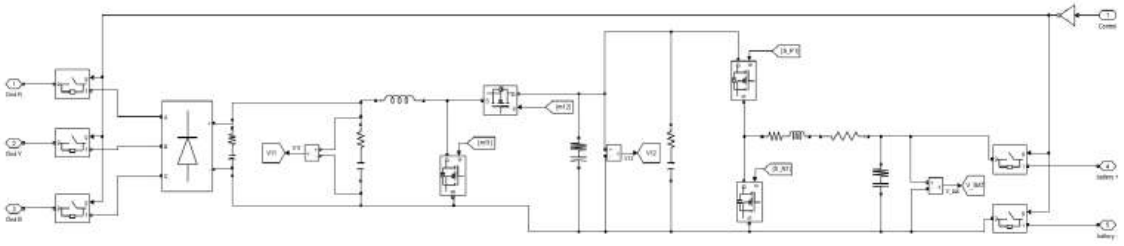

FIGURE 3.2: Simulation model of Charger box

The FFT of the grid current and the charging current is obtained as shown in figure 3.3 and figure 3.4 repectively. The THD in the grid current increases with increase in the number of EVs charging. A THD of 10.75 % and 13.92% in the grid current and charger current, respectively, for one EV connected to the grid is observed.

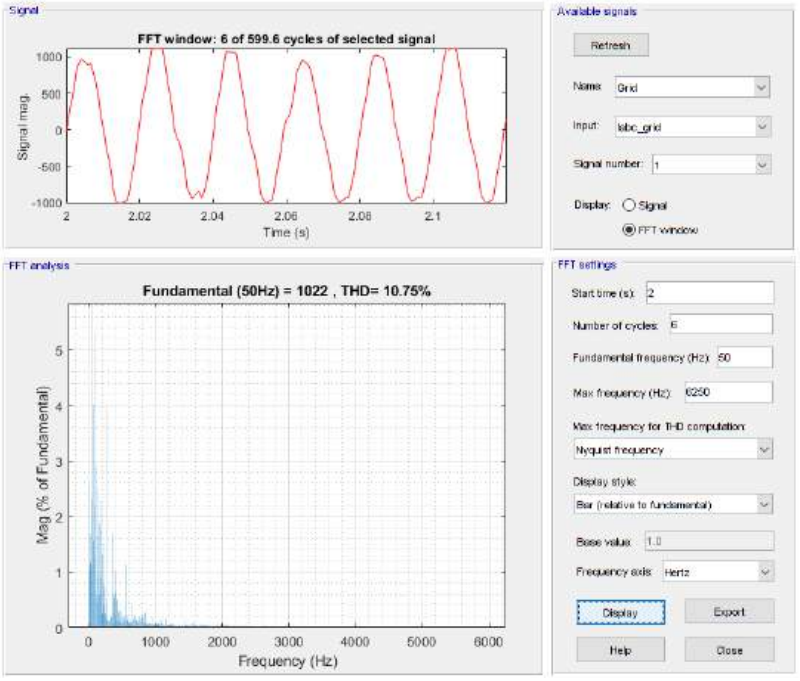

FIGURE 3.3: FFT of Grid Current

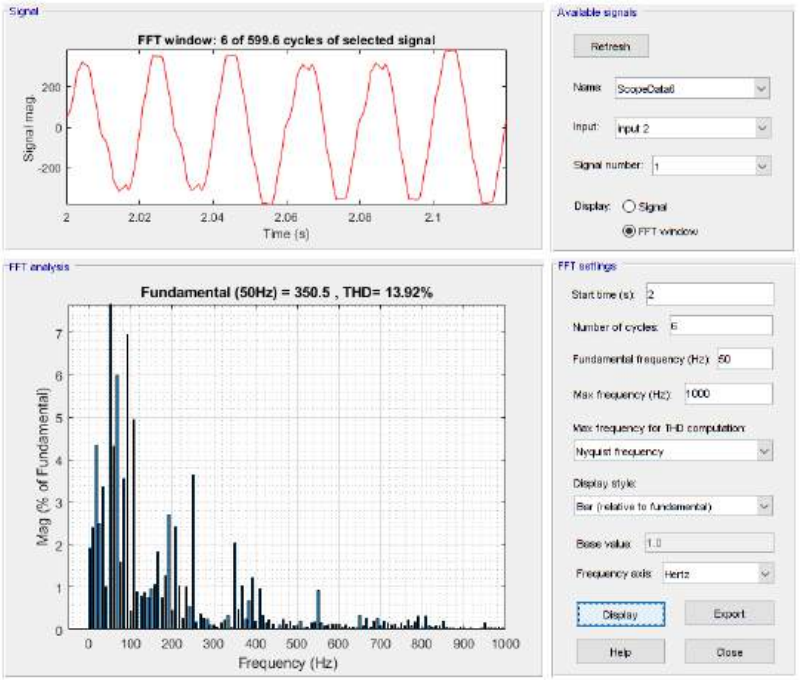

FIGURE 3.4: FFT of Charging Current

OPAL RT Simulation

A real-time analysis to verify the above results using OPAL-RT is carried out. OPAL-RT is a strong tool that is widely used for real-time simulation, hardware-in-the-loop (HIL) testing, and system validation across multiple sectors. The real-time simulation was carried out on the OPAL-RT Simulator. Figures 3.6 and 3.8 show the FFT of the grid current and charging current, respectively. It can be observed that there is significant distortion in the grid current profile and the current drawn by the EV charger.

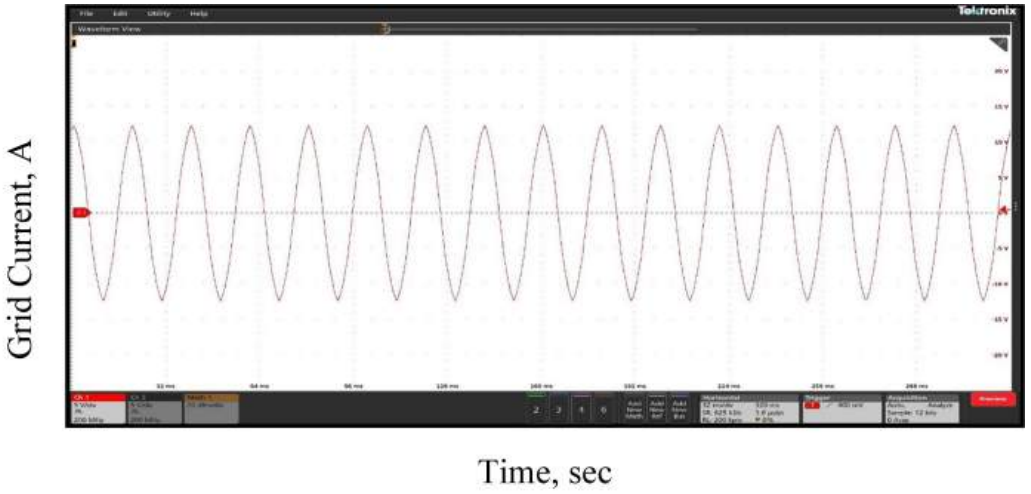

FIGURE 3.5: OPAL RT Waveform of Grid Current

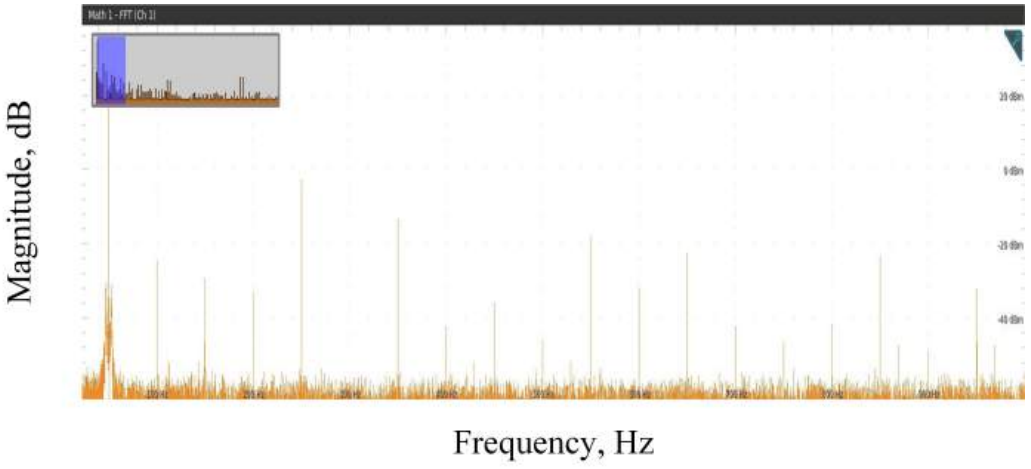

FIGURE 3.6: OPAL RT FFT of Grid Current

Observations using OPAL-RT have revealed a noticeable increase in Total Harmonic Distortion (THD) due to the charging of electric vehicles (EVs). This qualitative analysis

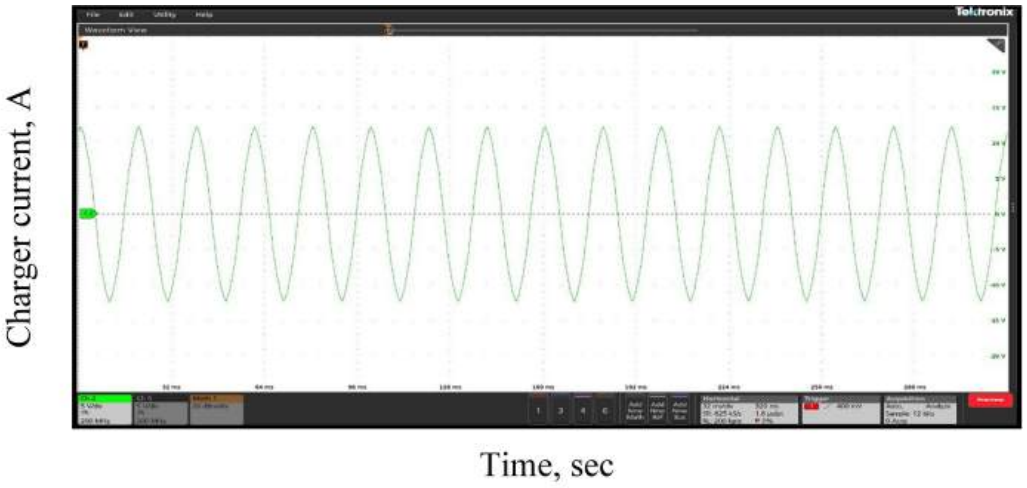

FIGURE 3.7: OPAL RT Waveform of Charging Current

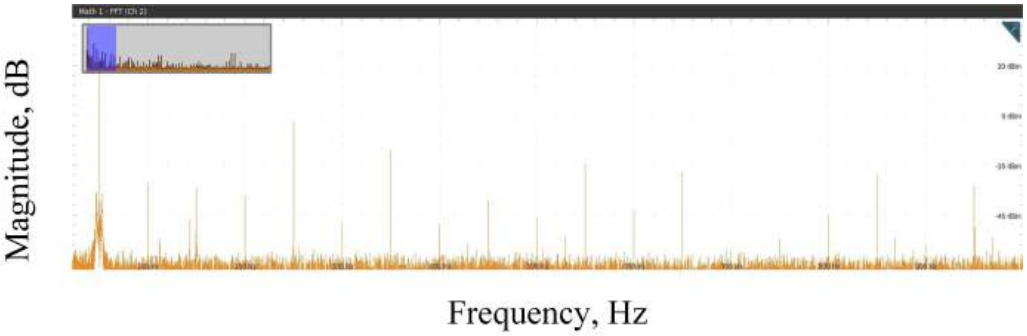

FIGURE 3.8: OPAL RT Charging Current FFT

aligns with the results obtained from MATLAB simulations, confirming the adverse impact of EV charging on power quality as shown in figures 3.6 and 3.8. The OPAL-RT real-time simulation platform provides a comprehensive view of the harmonic distortion introduced by EV chargers, highlighting the need for effective mitigation strategies to maintain grid stability and performance. These findings underscore the importance of addressing harmonics to ensure the reliable integration of EVs into the power grid.

3.2 Conclusion

Both MATLAB simulations and OPAL-RT observations consistently demonstrate that the increasing penetration of electric vehicles (EVs) leads to a significant rise in Total Harmonic Distortion (THD). This increase in THD adversely impacts power quality,

causing voltage and current distortions that can degrade the performance of electrical grid components. The alignment of results from both MATLAB and OPAL-RT underscores the reliability of these findings and highlights the critical need for effective strategies to mitigate harmonics.

From the above study it can be deduced that the charging of an EV through grid pollutes the power quality of the grid. In other words, electric vehicles (EVs) are becoming increasingly popular, but their charging demands negatively impact the power quality of the grid. Following points are concluded from the above analysis-

- **Increased THD:** The Total Harmonic Distortion levels rise due to the non-linear nature of EV chargers.
- **Voltage Fluctuations:** Frequent charging cycles cause voltage dips and spikes, affecting grid stability.

CHAPTER 4

SWITCHING CHARACTERISTICS OF THE MOSFET AND DOUBLE PULSE TEST

4.1 Introduction

MOSFETs are voltage controlled high speed devices. The SiC base MOSFETs are now widely used for various applications, particularly EV powertrain devices. With use of such devices, the power is inevitable. However to reduce the power loss, the primary cause for power loss need to be studied. The efficiency of the converters used in any application depends on the switching of these devices. The devices run by gate drivers.

Gate drivers are important component of the devices as it governs the functioning of the switches.

In order to find out the power loss in a mosfet it is important to understand its switching, because the power loss is Vds*Ids. The inverter output current i.i Ids which is the motor input current needs to be found out. It depends on the speed of the vehicle. A preliminary method has been has been identified as a part of the project.

4.2 Switching Characteristics of MOSFET

Conventionally, the MOSFETs are fed with voltage based pulses at the gate. The switching of a MOSFET is a dynamic process which involves the charging and discharging of the virtual capacitance between each terminal. Cgs is the capacitance between gate and source terminal, Cgd is the capacitance between gate to drain and Cds is the capacitance between drain and source. The capacitance vary inversely with the drain to source voltage. The turning on and off of the MOSFET switches is discussed in detail [15].

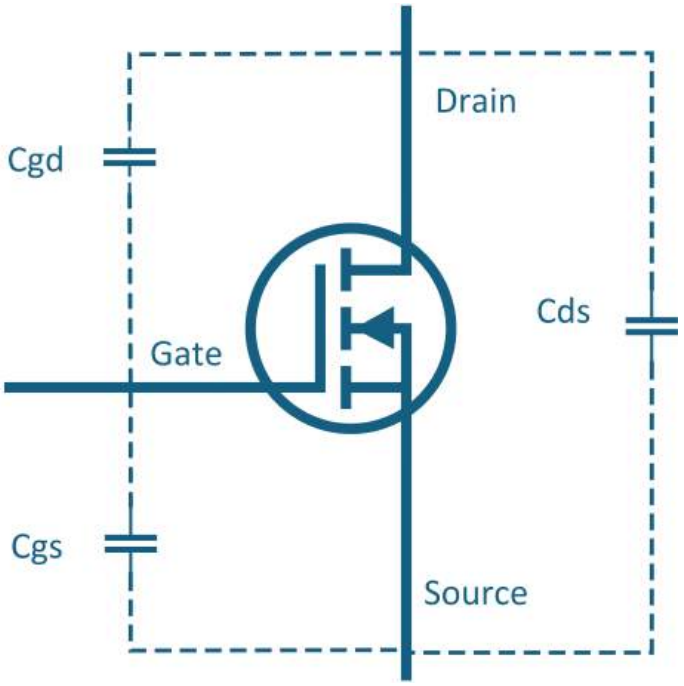

FIGURE 4.1: N-Channel MOSFET Symbol

During turn on

Figure 4.2 shows the variation in Vds and Id during the turn on of the MOSFET.

- At t1, Vgs is applied to the gate of the MOSFET. The input capacitance Cgs start charging
- During t2, when Vgs reaches threshold, the drain current Id starts rising and reaches maximum as Vgs reaches plateau.
- During time t3, the miller plateau volatge is attained. At plateau, the Cds discharges through load and Vds falls to minimum. In this situation the Cgs and Cgd are in parallel and charge to equal potential.
- During t4,as Vgs is increased further the capacitances Cgs and Cgd get charged further.

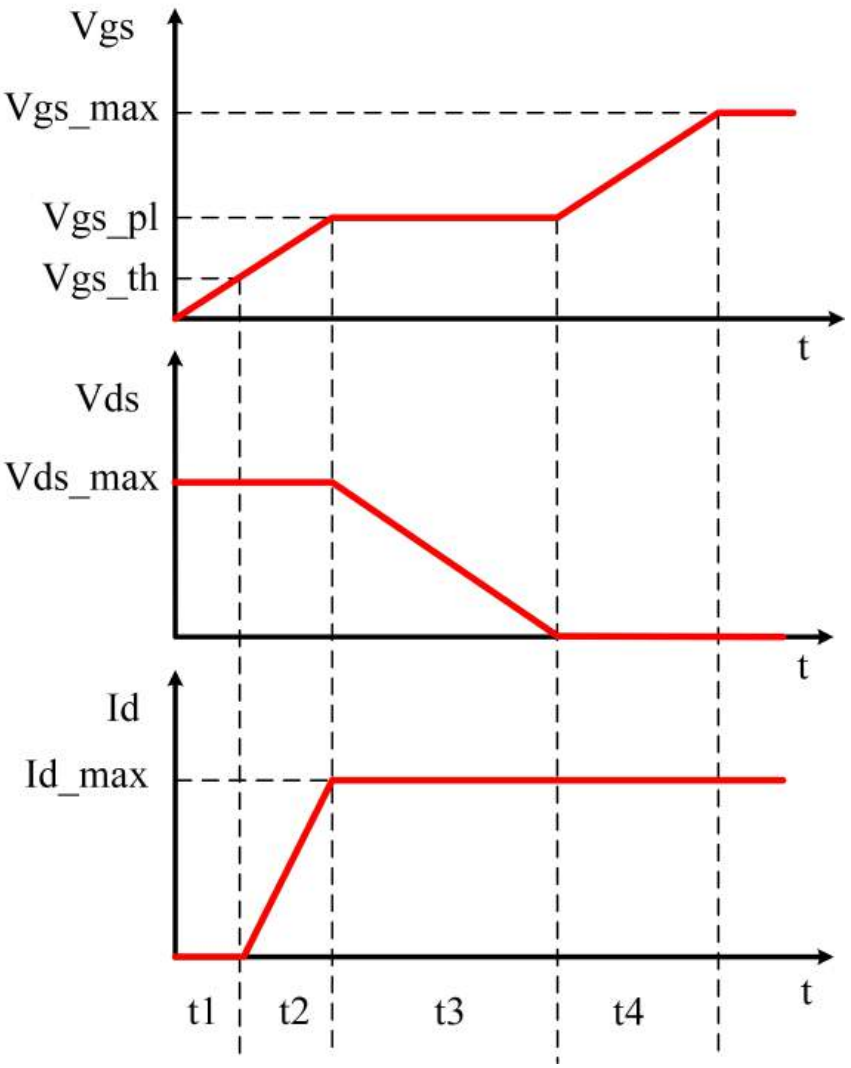

FIGURE 4.2: MOSFET Turn ON Characteristics

During turn off

Figure 4.3 shows the variation in Vds and Id during the turn off of the MOSFET.

- At t1, as Vgs starts decreasing, capcitances Cgs and Cgd start discharging till the miller plateau and Vds slightly increases.
- During t2, the miller plateau is achieved and Vds reaches maximum. Id remains unchanged.
- During t3, at the miller plateau, Vds rises to its maximum.

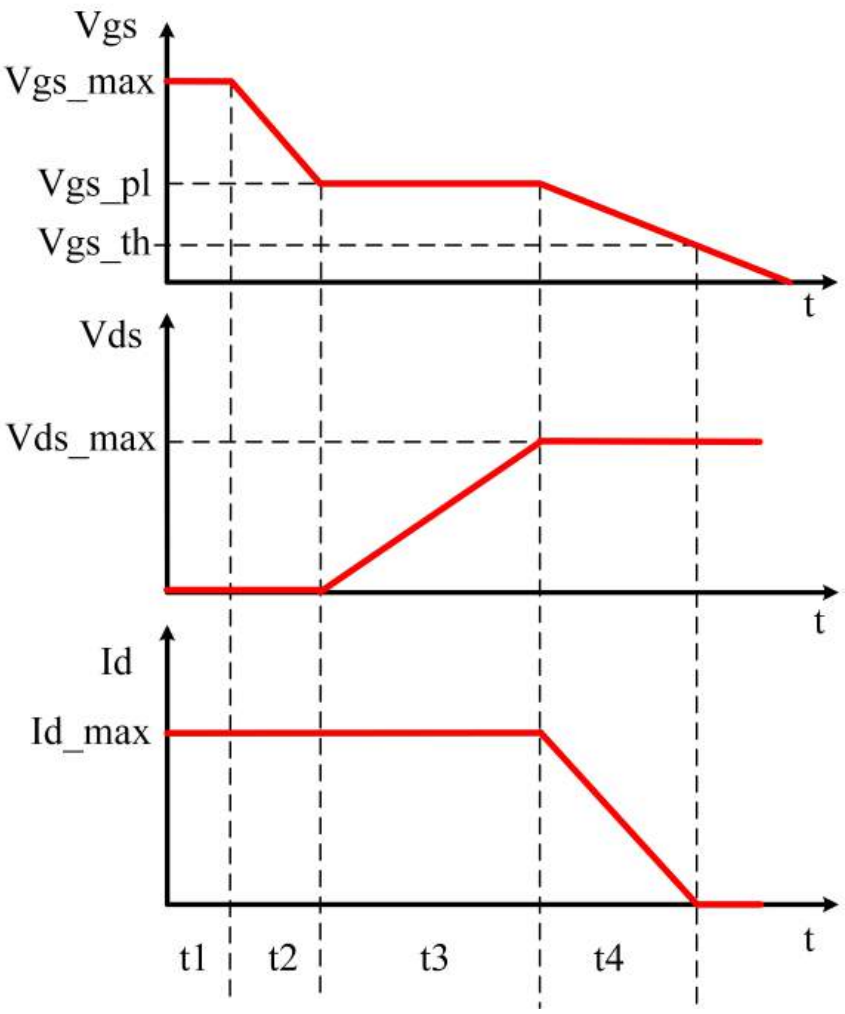

FIGURE 4.3: MOSFET Turn OFF Characteristics

- During t4 Now the Vgs further starts falling from the miller plateau which causes the drain current starts to fall and reaches almost zero.
- Lastly as the Vgs is further reduced to zero, the capacitance Cgs discharges completely. Vds and Id remain unchanged.

4.2.1 Overview of Power loss in MOSFET

During the switching operation of a MOSFET, following losses are incurred

- conduction loss (Pcond,sw),

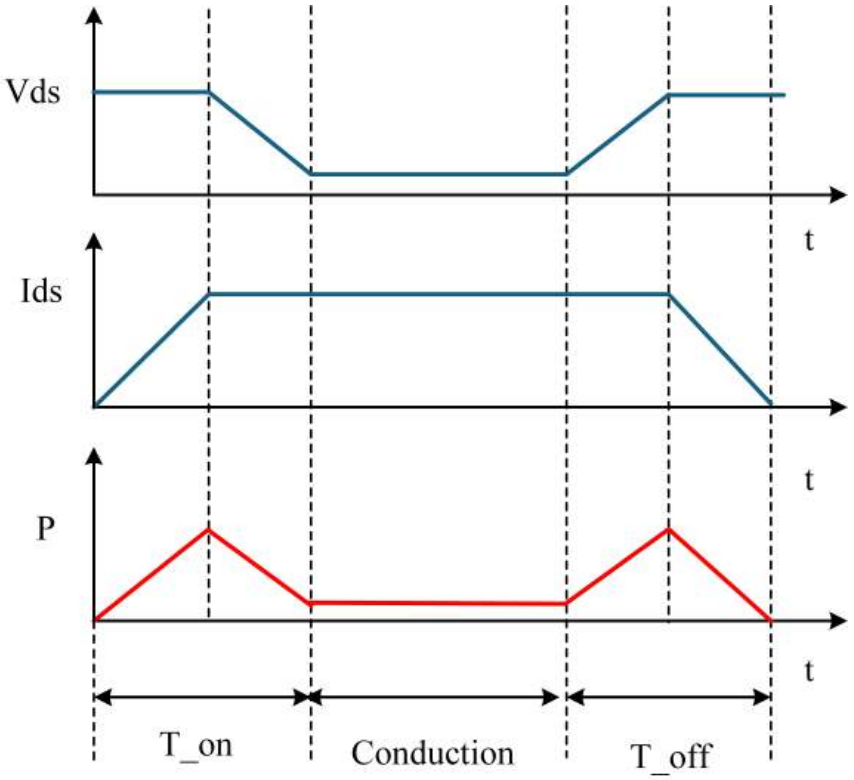

FIGURE 4.4: Power loss in MOSFET

- switching loss (Psw,Sw), and
- stray losses (Ps) (very less and negligible)

The total power loss in a MOSFET switch is the sum total of these individual losses.

$$P_{Total} = P_{cond,sw} + P_{sw,Sw} + P_s \tag{4.1}$$

The equation 4.1 gives the total power loss in the switch.

Conduction losses

Conduction losses in the MOSFET switch can be calculated using equation

$$P_{cond} = R_{DSON} * I^2_{Drms} \tag{4.2}$$

Where RDSON and IDRMS are the drain-source on-state resistance and the drain-to-source current, respectively. RDSON can be obtained from the datasheet of the module. The conduction losses are assumed to be constant, since the switching frequency is high, the conduction period is very small and the drain current is constant. Also the resistance Rdson is dependent on the temperature hence it is also constant at a given instant.

Switching losses

Figure 5 shows that there is power loss in the switch during switching transitions Total switching loss in the switch

$$P_{sw} = (E_{ON} + E_{OFF}) * f_{sw} \tag{4.3}$$

Where Eon and Eoff are the energy losses in Joules during turn on and turn off respectively. Fsw is the switching frequency in Hz.

Total Power loss in the three-phase traction inverter is

$$P_{loss} = 6 * P_M \tag{4.4}$$

Hence, the efficiency of the inverter is given by

$$\eta_{inv} = \frac{P_o}{P_o + P_{loss}} * 100 \tag{4.5}$$

Where Po is the output power of the inverter. The above switching characteritcs is when the MOSFET is fed with the voltage pulses at the gate.

4.3 Double Pulse Test

A double pulse test is conducted to measure energy loss during device turn-on and turn-off, as well as reverse recovery parameters.The double pulse test is a crucial method used to evaluate the switching performance of power MOSFETs (Metal-Oxide-Semiconductor Field-Effect Transistors). This test helps engineers understand how the MOSFET behaves under different conditions, particularly focusing on its switching characteristics, efficiency, and potential issues like voltage spikes and oscillations.

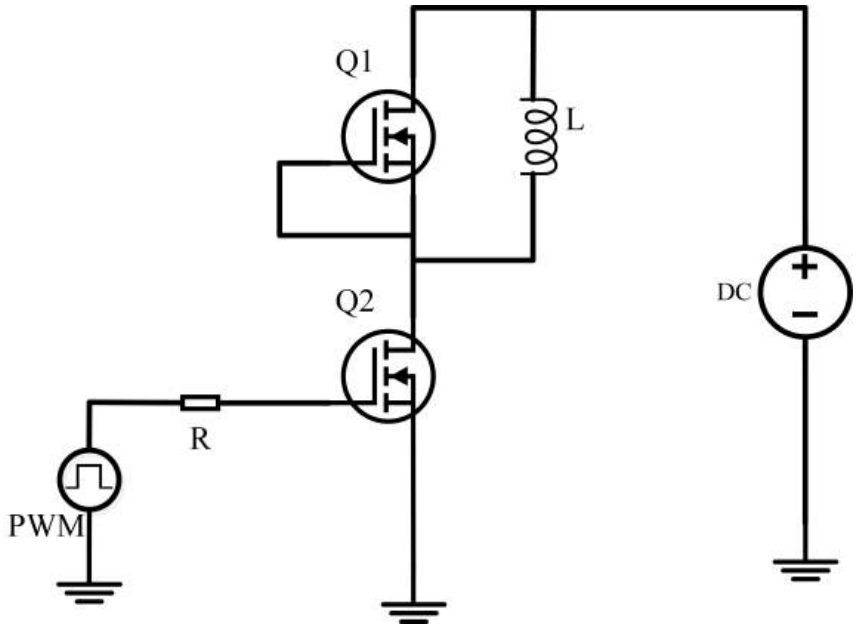

FIGURE 4.5: Double Pulse Test Circuit Diagram

In figure 4.5, the MOSFET Q2 is the Device Under Test (DUT). The DUT MOSFET is placed in a test circuit, typically involving an inductive load, a gate driver, and measurement equipment to monitor voltage and current as shown in figure 4.5. A programmable pulse generator is used to create two consecutive pulses. The first pulse turns the MOSFET DUT on, allowing current to flow through the inductive load. The second pulse, after a short delay, turns the MOSFET Q2 on again to simulate switching conditions.

Procedure

1. First Pulse : The DUT is turned on, and current builds up in the inductive load.
2. Off Period : The DUT is turned off, and the current circulates through the freewheeling diode.
3. Second Pulse : The DUT is turned on again, and the current flow resumes.
4. The voltage and current waveforms are recorded and analyzed to identify switching losses, voltage spikes, and oscillations.

This test is essential for ensuring the reliability and efficiency of MOSFETs in power electronics applications.

Result analysis

Measurement Parameters

- Switching Times : The test measures the turn-on and turn-off times of the MOSFET. They are defined as follows,

  Turn-on delay time is the time interval between 10% of the rising VGS and 90% of the dropping IDS.

  Rise time is the time interval where the drain-source current (IDS) rises from 10% and 90% of the IDS.

$$t_{on} = t_{don} + t_r \tag{4.6}$$

  Turn-off delay time is the time interval between 90% of the dropping VGS and 90% of the rising IDS.

  Fall time is the time interval where the drain-source current (IDS) falls from 10%

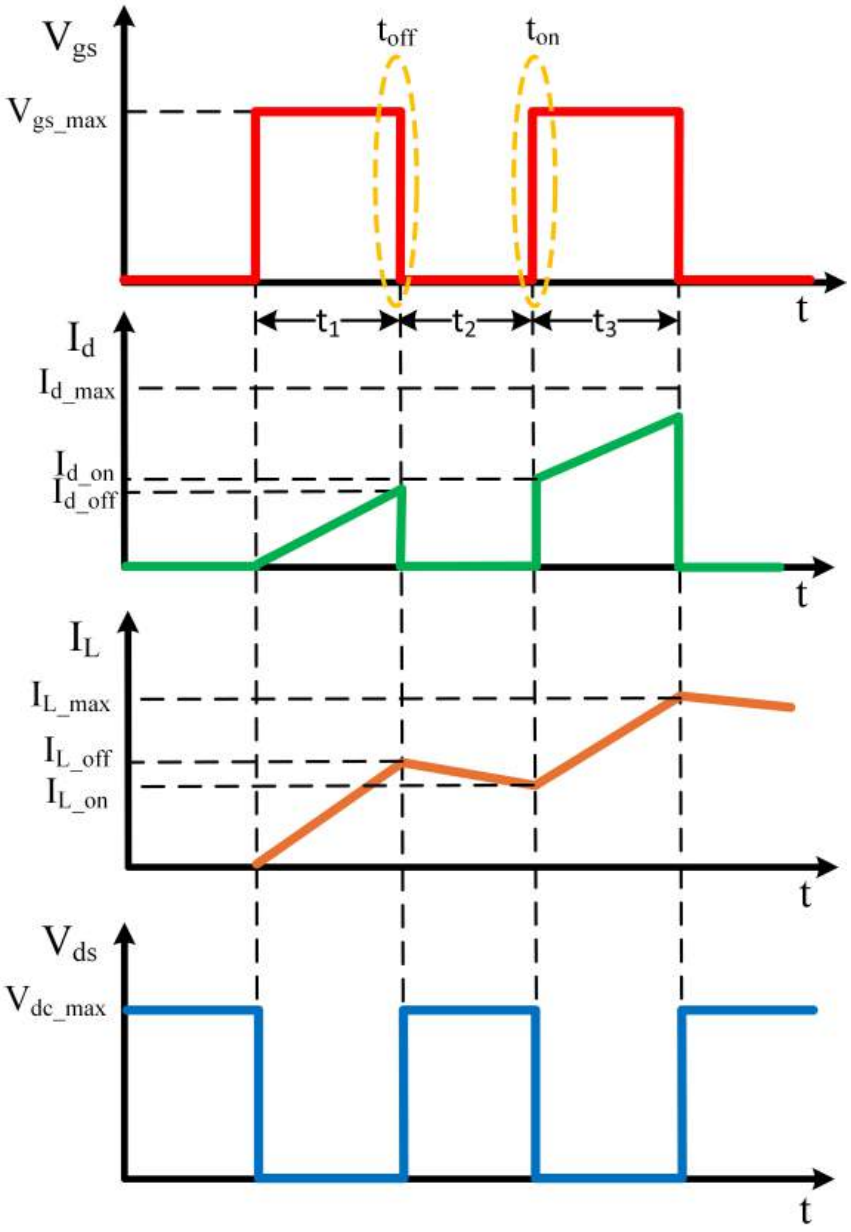

FIGURE 4.6: Results of the Double Pulse Test

and 90% of IDS.

$$t_{off} = t_{doff} + t_f \tag{4.7}$$

- Switching Energy : It evaluates the energy losses during switching. The switching

energy is the integral of the power dissipated during turn-on and turn-off of a semiconductor.

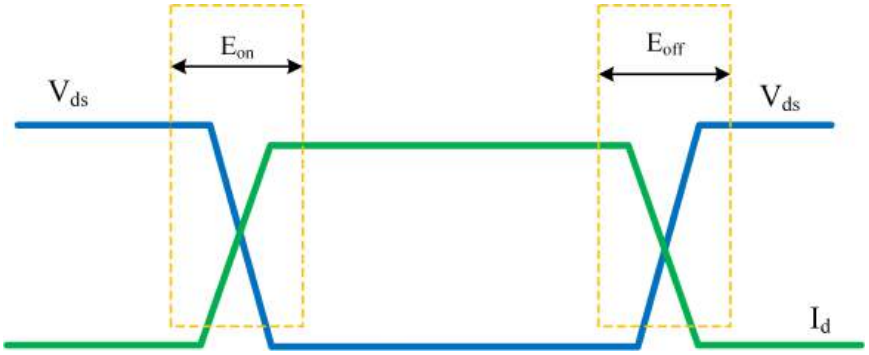

FIGURE 4.7: Switching Energy Loss

- Reverse Recovery Characteristics : If a freewheeling diode is used, its reverse recovery behavior is also analyzed.

4.4 Conclusion

This chapter discusses the switching characteristics of MOSFETs, including their power losses and the double pulse test. It provides a comprehensive analysis of how these factors affect the performance and efficiency of MOSFETs in power electronics applications.

CHAPTER 5

CURRENT ESTIMATION AND SWITCHING TIME ANALYSIS

5.1 Introduction

Primarily, battery, a traction inverter and a motor are required in the electric vehicle powertrain for the vehicle to move. The traction inverter is the heart of this operation where it converts DC from the battery to AC for the motor.

The current drawn by the motor depends on the speed of the vehicle. Therefore, the performance of the traction inverter is dependent on the speed with which the vehicle is moving. The movement of the vehicle is also dependent on factors such as aerodynamic drag, rolling resistance, rotational losses etc. These parameters are defined by respective coefficients called coast down coefficients are estimated by coast down test done on the vehicles. The traction torque developed on the motor is directly proportional to the motive torque that sets the vehicle in motion.

5.2 Vehicle dynamics

A preliminary approach has been defined to find the inverter output current from the speed of the vehicle for power loss estimation. To estimate the performance of the traction inverter, the driving cycle of the vehicle should be known. The Worldwide Harmonized Light Vehicle Test Procedure i.e. WLTP has standardized vehicles depending on the vehicle unladen mass and the vehicle speed. The Worldwide Harmonised Light vehicles Test Procedure (WLTP) is a global driving cycle standard for determining the levels of pollutants, CO2 emission standards and fuel consumption of conventional internal combustion engine (ICE) and hybrid automobiles, as well as the all-electric range of

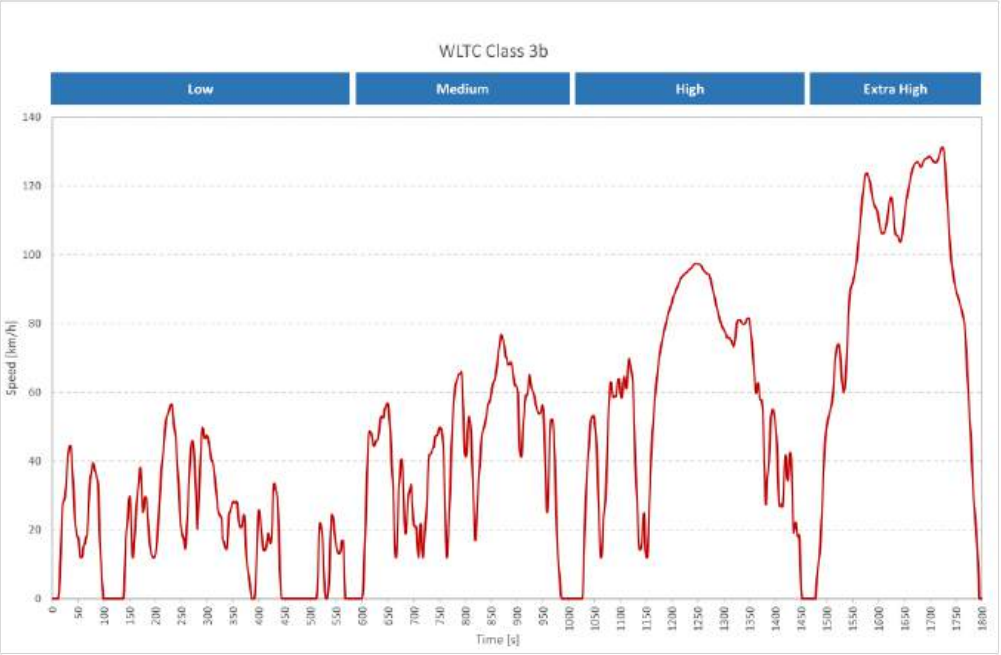

FIGURE 5.1: WLTC Class 3b Drive Cycle

plug-in electric vehicles. The vehicles are classified based on the weight and speed of the vehicle. For Class 3b vehicles, the ratio is greater than 34. The drive cycle for class 3b vehicle shown in figure 3 covers a distance of approximately 23 km in half an hour with maximum speed reaching up to 131 kmph.

5.2.1 Current Profile Estimation

For the current profile estimation, the WLTP class 3b vehicle is considered. **Aerodynamic drag (FD)** is the resistance of air to the movement of vehicles. The **rolling resistance (FR)** is the combination of all frictional load forces due to the deformation of the tire on the road surface and the friction within the drivetrain. The **motive force (F)** required to accelerate the vehicle is the sum of the acceleration, load, and climbing forces.

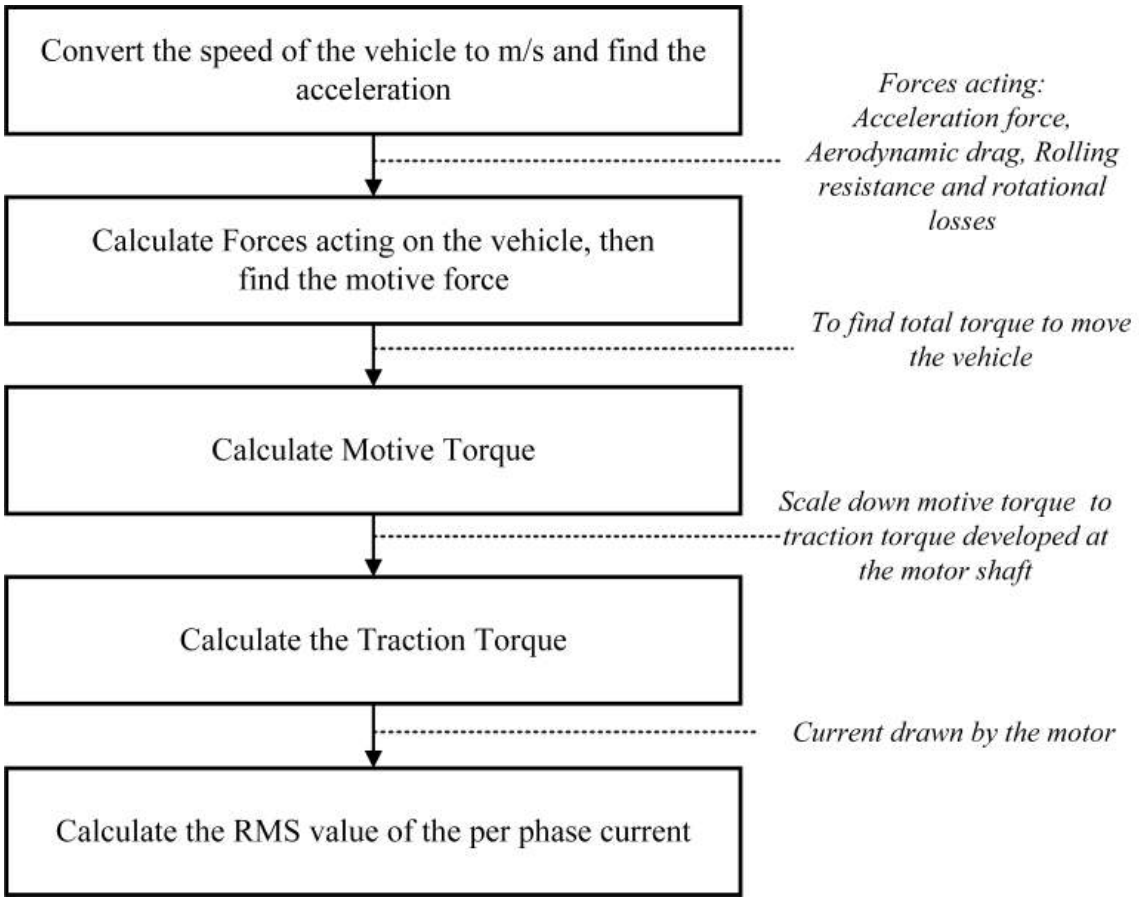
Convert the speed of the vehicle to m/s and find the acceleration
Forces acting: Acceleration force, Aerodynamic drag, Rolling resistance and rotational losses
Calculate Forces acting on the vehicle, then find the motive force
To find total torque to move the vehicle
Calculate Motive Torque
Scale down motive torque to traction torque developed at the motor shaft
Calculate the Traction Torque
Current drawn by the motor
Calculate the RMS value of the per phase current

FIGURE 5.2: Procedure to estimate the current profile

The WLTC Drive cycle is known for class 3b vehicle. To find the current profile from the speed profile, the following method is used. Speed is known at each time in kmph, convert it to m/s (by dividing it by 3.6). To find the acceleration of the vehicle at each instant, apply Newton's first equation of motion,

$$Final\ velocity = Initial\ velocity + acceleration * time \tag{5.1}$$

Rearranging the equation 5.1, we get the acceleration (in m/s^2)

$$acceleration\ (a) = \frac{Final\ velocity\ (v) - intial\ velocity\ (u)}{time} \tag{5.2}$$

The motive force describes the force required for linear motion. It is calculated by

$$F = m * a + A + B * v + C * v^2 \tag{5.3}$$

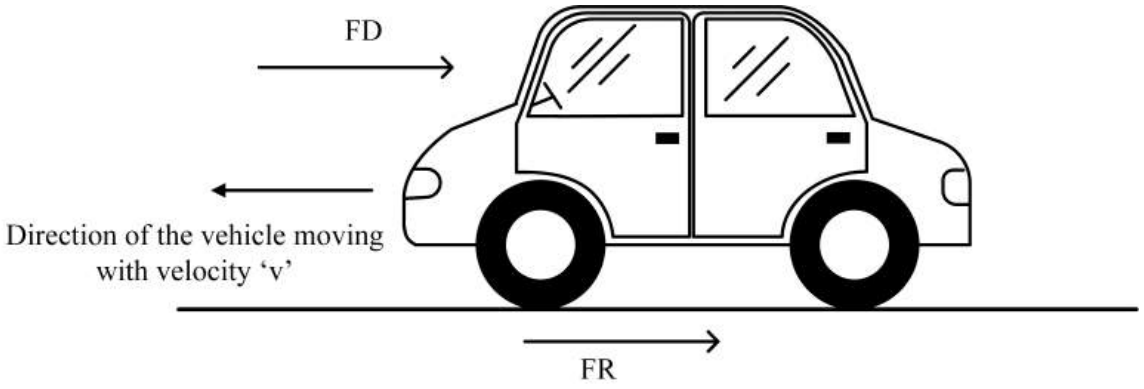

FIGURE 5.3: Forces acting on the moving vehicle

where m is mass in kg and a is acceleration in m/s^2, A is the Coefficient of Rolling resistance in N, B is the Coefficient of Rotational losses in N/m/s, C is the Coefficient of Aerodynamic drag in N/(m/s)^2 and v is the velocity of the vehicle. The motive torque (T_m) is the torque required at the drive axle and is obtained by multiplying the motive force by the wheel radius r, thus relating the linear motion to rotating motion. The Motive torque (T_m) (Nm) is given as

$$T_m = F * r \tag{5.4}$$

where F is motive force and r is the radius of the wheel. From Newton's second law of motion for a rotating system, the torque is given as

$$T = J\alpha \ = \ J^{d\omega}/_{dt} \tag{5.5}$$

where J is the moment of inertia, and ω and α are the angular speed and acceleration. In addition to the motive torque to move the vehicle, we must also consider the torque to spin the rotating parts within the drivetrain. This is represented by a drive-axle referenced moment of inertia, J_{axle}. Thus, the total torque required at the drive axle T_{axle} is the sum of the motive torque and the torque required to accelerate J_{axle}:

$$T_{axle} = T_m \ + \ J_{axle}\alpha_{axle} \tag{5.6}$$

where α_{axle} is the angular acceleration. In this case, neglect the inertial force. The traction torque (T_t) is the torque developed on the output shaft of the electric motor. The traction

torque is directly geared to the drive-axle torque. The gearing and transmission efficiency can significantly impact the required motive torque. The axle torque is related to the traction torque, when motoring, as follows: Therefore, the motive torque (Tm) = axle torque (Taxle).

$$T_{axle} = \eta_g * n_g * T_t \tag{5.7}$$

where η_g and n_g are the gear efficiency and gear ratio respectively. The above equation gives the traction torque developed at the motor shaft [16]. The above equation gives the traction torque developed at the motor shaft.

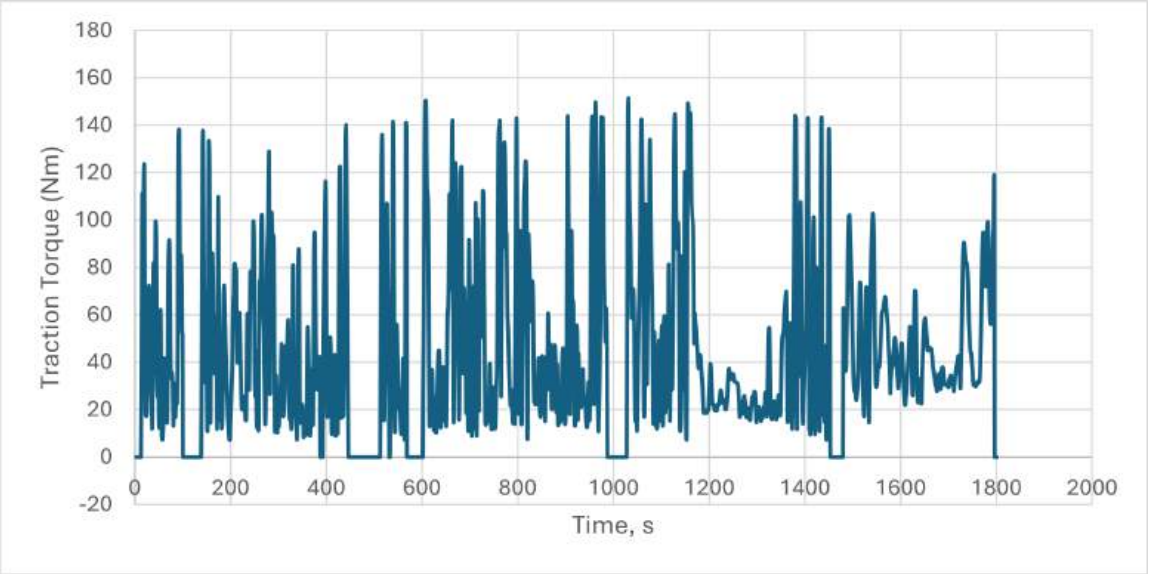

FIGURE 5.4: Traction Torque vs Time

The motor current is directly proportional to the traction torque. Hence to calculate the per phase current,

$$T_t = 3 * k * I_{ph} \tag{5.8}$$

where, k is the machine constant and I_ph is the rms value of the per phase current.

Furthermore, the angular speed of the motor (in rad/s) can be calculated by

$$\omega_r = \frac{v}{r} * n_g \tag{5.9}$$

where ω_r , n_g , v are the angular velocity of the motor, gear ratio and linear velocity of the vehicle, respectively. The input power (P, Watts) to the motor is the product of the traction

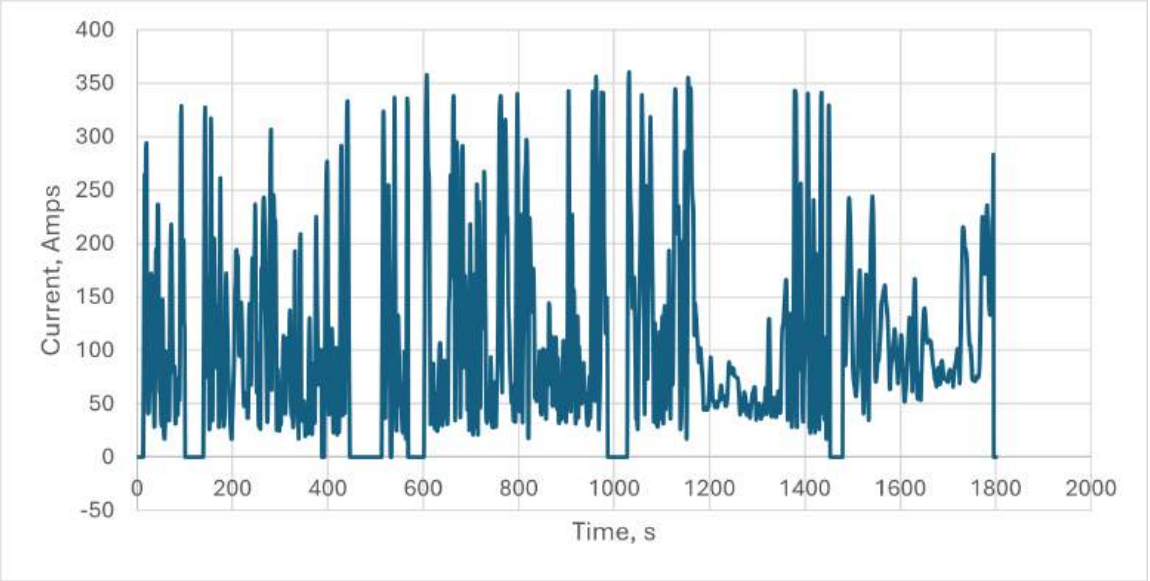

FIGURE 5.5: Current vs Time

torque (T_t) and angular speed of the motor (ω_r)

$$P = T_t * \omega_r \tag{5.10}$$

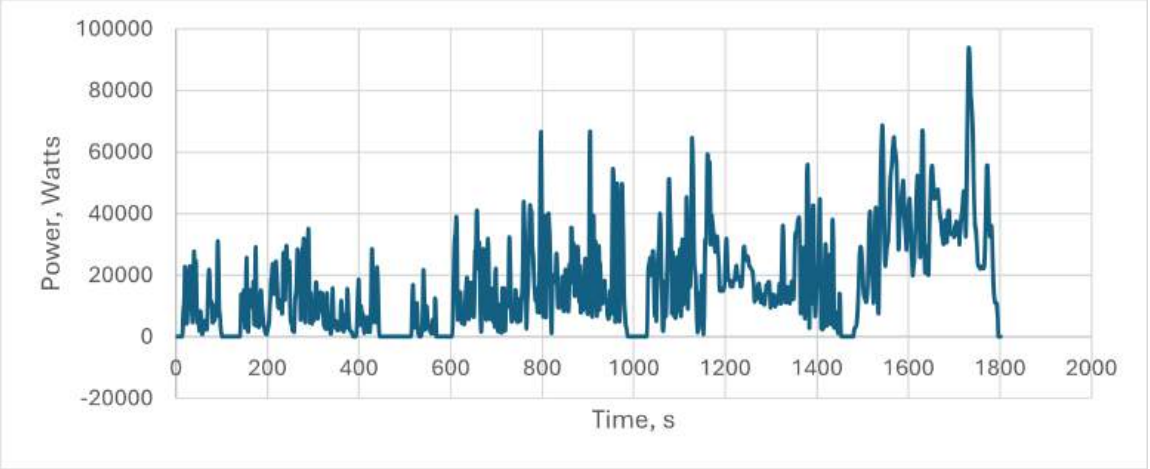

FIGURE 5.6: Power vs Time

The following equation gives the Back emf, denoted by E_{ph} (Volts),

$$E_{ph} = k * \omega_r \tag{5.11}$$

where k is a machine constant The rotor frequency f_r (Hz) is given by

$$f_r = \frac{\omega_r}{2\pi} \tag{5.12}$$

The electrical input frequency (f_e) is given by

$$f_e = \frac{p}{2} * f_r \tag{5.13}$$

The above calculations are useful for the vehicle moving on a horizontal road. For the vehicle moving on a slope, the gradability component (mgsin$theta$) gets added to the motive force calculations.

5.2.1.1 Sample Calculation

It is to be noted that the values of coast down coefficients A, B and C are taken from a technical article published by A and D, where a coast down test on a vehicle was conducted and these coefficients were estimated. Therefore, the values of these coefficients are subject to change. These coefficients are different for each vehicle. In this case it is assumed that the coefficients A, B and C are 191.69 N, 2.54 N/m/s, 0.41 N/(m/s)^2 respectively.

TABLE 5.1: Values considered

Variables	**Symbol**	**Value**	**Units**
Coefficient A correlates to the rolling resistance	A	191.69	N
Coefficient B relates to the spinning or rotational losses	B	2.54	N/m/s
Coefficient C relates to the aerodynamic drag	C	0.41	N/(m/s)^2
Mass of the vehicle (BMW i7 eDrive50)	m	2595	Kg
Radius of the wheel (BMW i7, 245/50 R19)	r	0.36	m
Machine constant (Assumed)	k	0.14	V/rad/s
Gear ratio	ng	10.28	
Gear efficiency	η_g	1	
Poles	p	8	
Acceleration	a	1.19	m/s^2
Velocity	v	4.69	m/s

TABLE 5.2: Calculation of Various Forces

Forces Calculation			
Acceleration force (Fa)	m*a	3088.05	N
Aerodynamic drag (Fd)	$C*v^2$	9.035502	N
Rolling Resistance (Fr)	A	191.69	N
Spinning/Rotational Losses (Fl)	B*v	11.92389	N
Road-load force ($F=ma+A+Bv+Cv^2$)	F	3300.699	N
Torque Calculation			
Motive Torque (Tm)	F*r	1188.252	Nm
Traction Torque (Tt)	Tm/ng*ng	115.5887	Nm
Current Calculation			
Per Phase Current (Iph)	Tt/3k	275.2112	A

5.2.2 Rise time and Fall time Calculation

As discussed earlier in this chapter, it is evident that the power loss in the MOSFET is dependent on the virtual capacitances between the terminals of the MOSFET. The turn on and turn off times are dependent on various parmeters such as drain current, gate drive strength, gate current, etc.

5.2.2.1 When Vgs is applied

The capcitance Cgd is inversely proportional to the drain-to-source voltage Vds i.e. when Vds increases, Crss = Cgd decreases and *vice-versa* as shown in figure 5.7 .

$$i_g = C_{rss}\frac{dV}{dt} \tag{5.14}$$

- **Vds fall time calculation**

  Since the gate-drain capacitance (Cgd) varies non-linearly with respect to the drain-source voltage (Vds), the Vds fall time is divided into segments where the reverse transfer capacitance (Crss) is considered constant within each segment, as shown in the figure 5.8 .

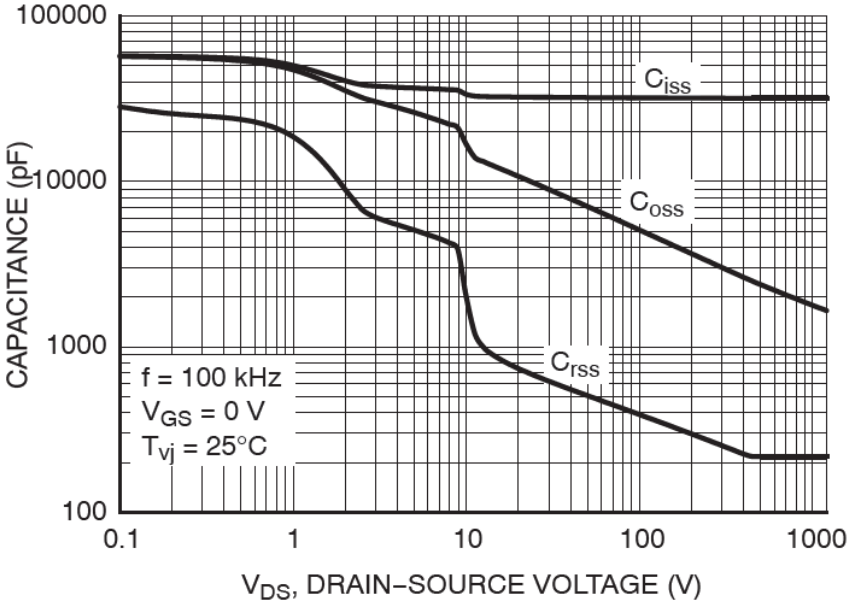

FIGURE 5.7: Typical Capacitance vs Drain-Source Voltage (Vds)

For the turn on, the current ig is given by

$$i_g = \frac{V_{pl} - V_{th}}{R_{gon}} \tag{5.15}$$

Substitute equation 5.15 into equation 5.14, along with the corresponding dV and Crss values, to calculate the fall time of Vds. Therefore the fall time of Vds is given by

$$t_{fu} = (V_{dd} - V_{ds}) \frac{R_{gon} C_{rss}}{V_{gs} - Vpl} \tag{5.16}$$

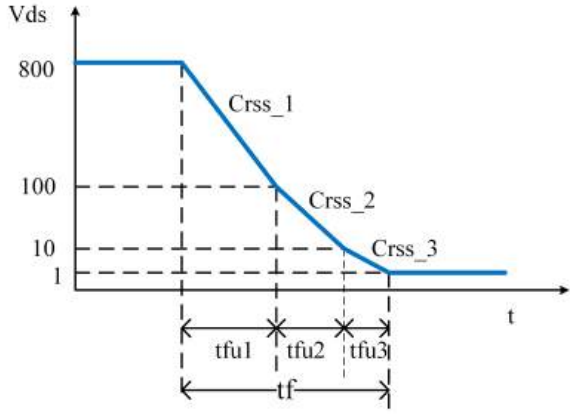

FIGURE 5.8: Vds fall time

The total fall time is the sum of the times of each segment.

$$t_f = t_{fu1} + t_{fu2} + t_{fu3} \tag{5.17}$$

- **Vds rise time calculation**

  During turn-off, Vds begins to rise. Since the discharge of Crss is non-linear, it is divided into three segments, as illustrated in figure 5.9.

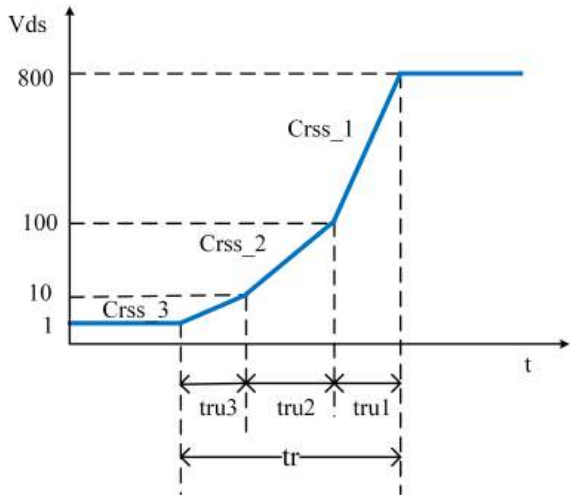

FIGURE 5.9: Vds Rise time

For the turn off, the current ig is given by

$$i_g = \frac{V_{pl} - V_{th}}{R_{goff}} \tag{5.18}$$

Substitute equation 5.18 into equation 5.14, along with the corresponding dV and Crss values, to calculate the rise time of Vds. Therefore the rise time of Vds is given by

$$t_{ru} = (V_{dd} - V_{ds}) \frac{R_{goff} C_{rss}}{V_{gs} - Vpl} \tag{5.19}$$

The total rise time is the sum of the times of each segment, given by equation 5.20.

$$t_r = t_{ru1} + t_{ru2} + t_{ru3} \tag{5.20}$$

- **Rise time and fall time of Id**

When the Vgs rises from threshold to the miller voltage, the drain current rises to maximum. During this period the capacitance Cgs is charging and Cds is constant. Therefore to find the rise time of the Ids we need to find the rise of Vgs from the threshold (Vth)to miller voltage (Vpl).

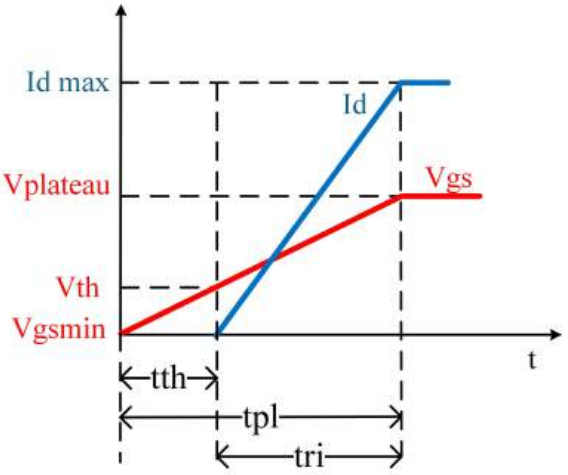

FIGURE 5.10: Rise time of Id

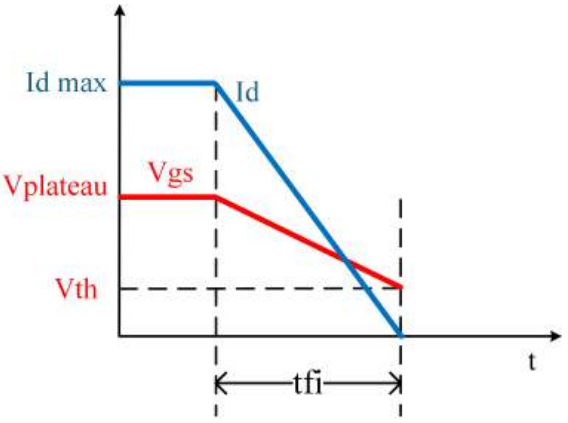

FIGURE 5.11: Fall time of Id

$$ln\frac{V_s - V_c}{V_s - V_o} = \frac{-t}{RC} \tag{5.21}$$

The gate-source capapcitance Cgs initially has a voltage Vo. When the device turns ON, the gate-source voltage Vgs starts at Vgsmin. Conversely, during turn off, Vgs starts at Vpl. The rise time and fall time of the current can be determined by substituting the initial voltage across the Cgs in equation 5.21.

5.2.2.2 When ig is applied

When a current-based pulse is applied to the device, the gate-source voltage Vgs rises linearly rather than exponentially. This linear behavior occurs because the gate current is actively controlled during switching. As a result, the rise and fall times of the drain current Id can be determined using 5.22.

To determine the rise and fall times of the drain-source voltage Vds, the same procedure used for voltage source gate driver can be followed. However, in this case, the gate current ig is held constant. The rise and fall behaviour of the V_{ds} and I_d is same as shown in figures 5.8,5.9, 5.10 and 5.11.

$$i = C\frac{dV}{dt} \tag{5.22}$$

5.2.3 Sample Calculation

A sample calculation to determine the rise and fall times of the Vds and Id is as follows.

When V_{gs} is applied

When the MOSFETs are given V_{gs} pulses, an external resistor is required to limit the ringing effect. However it limits the switching frequency, increases the switching times of the device and contribute to losses.

Parameter	Value	Unit
V_{dd}	800	V
R_{gint}	2.1	ohm
R_{gext}	3	ohm
$V_{plateau}$	8.3	V
C_{rss1}	310	pF
C_{rss2}	1200	pF
C_{rss3}	11000	pF

V_{ds} Fall and Rise time calculations

During turn on the Vds falls as shown in figure 5.8 while Vds rises during turn off as shown in figure 5.9. Following tables show the calculations of the fall time and rise time of the V_{ds}.

V_{ds} **Fall Time Calculation**		
Parameter	Value	Unit
V_{gs}	20	V
R_{gon}	5.1	ohm
V_{ds_on}	1	V
V_{ds_2}	100	V
V_{ds_3}	10	V
$V_{dd} - V_{ds\_2}$	700	V
$V_{ds\_2} - V_{ds\_3}$	90	V
$V_{ds\_3} - V_{ds\_on}$	9	V
$V_{gs} - V_{plateau}$	11.7	V
i_g	2.3	A
Δt_{fu1}	94.59	ns
Δt_{fu2}	47.08	ns
Δt_{fu3}	43.15	ns
t_{fu}	184.82	ns

V_{ds} **Rise Time Calculation**		
Parameter	Value	Unit
V_{gs}	-5	V
R_{goff}	3.1	ohm
V_{ds_on}	1	V
V_{ds_2}	100	V
V_{ds_3}	10	V
$V_{dd} - V_{ds\_2}$	700	V
$V_{ds\_2} - V_{ds\_3}$	90	V
$V_{ds\_3} - V_{ds\_on}$	9	V
$V_{gs} - V_{plateau}$	11.7	V
i_g	3.8	A
Δt_{ru1}	57.50	ns
Δt_{ru2}	28.62	ns
Δt_{ru3}	26.23	ns
t_{ru}	112.34	ns

I_{ds} Rise time calculation

When I_d is rising, V_{gs} increases from V_{th} to V_{pl}. The gate-source capacitance C_{gs} begins charging from its initial voltage. Therefore, the time required to charge C_{gs} from the initial voltage to the threshold, and from the initial voltage to the plateau, is calculated separately. Since the drain current I_d starts to rise as V_{gs} increases from the threshold voltage V_{th} to the plateau voltage V_{pl}, the rise time is defined as the difference between these two charging times, as shown in figure 5.10. These values are presented in the following tables.

Parameter	Value	Unit
R_{gint}	2.1	ohm
R_{gext}	3	ohm
R_g	5.1	ohm
C_{iss} at V_{ds} = 400V	31.7	nF
C_{rss} at V_{ds} = 400V	220	pF
$C_{gs} = C_{iss} - C_{rss}$ at $V_{ds} = 400$V	31.48	nF
$R \cdot C$	1.61×10^{-7}	

V_{gs} **Rise till** V_{pl}		
Parameter	Value	Unit
V_o	-5	V
V_s (V_{gs})	20	V
$V_c(t)$	8.3	V
$V_s - V_c(t)$	11.7	V
$V_s - V_o$	25	V
$\ln\left(\frac{V_s - V_c(t)}{V_s - V_o}\right)$	0.76	
t_{pl}	1.22×10^{-7}	sec

V_{gs} **Rise till** V_{th}		
Parameter	Value	Unit
V_o	-5	V
V_s (V_{gs})	20	V
$V_c(t)$	3.2	V
$V_s - V_c(t)$	16.8	V
$V_s - V_o$	25	V
$\ln\left(\frac{V_s - V_c(t)}{V_s - V_o}\right)$	0.40	
t_{th}	6.38×10^{-8}	sec

I_{ds} **Rise Time Calculation**		
Parameter	Value	Unit
$t_{ri} = t_{pl} - t_{th}$	58.08	ns

I_{ds} Fall time calculation

Similarly, during turn-off, the drain current I_d decreases as the gate-source voltage V_{gs} falls from the plateau voltage V_{pl} to the threshold voltage V_{th} as shown in figure 5.11, and it is calculated as shown in the following table.

Parameter	Value	Unit
R_g	3.1	ohm
$C_{gs} = C_{iss} - C_{rss} at V_{ds}$ = 400V	31.48	nF
$R_g \cdot C_{gs}$	9.76×10^{-8}	

I_{ds} **Fall Time Calculation**		
Parameter	Value	Unit
V_o	8.3	V
V_s (V_{gs})	-5	V
$V_c(t)$	3.2	V
$V_s - V_c(t)$	-8.2	V
$V_s - V_o$	-13.3	V
$\ln\left(\frac{V_s - V_c(t)}{V_s - V_o}\right)$	0.48	
t_{fi}	47.20	ns

The turn on time (t_{on}) and turn off time (t_{off}) when V_{gs} is applied is calculated as,

	Parameter	**Value**
Turn on time	$t_{on} = tfu + tri$	242.91 ns
Turn off time	$t_{off} = tru + tfi$	159.54 ns

Power Loss With Voltage source driver

Now, the power loss during switching transitions when V_{gs} is applied is calculated as,

TABLE 5.3: Switching Parameters and Energy Calculations when Vgs is applied

Parameter	**Value**	**Unit**
Vds	800	V
Id	400	A
Switching frequency (fsw)	10	kHz
Eon	$V_{ds} I_{ds} t_{on}$	38.86 mJ
Eoff	$V_{ds} I_{ds} t_{off}$	25.53 mJ
P_{sw}	$(E_{on} + E_{off}) \cdot fsw$	643.91 W

When i_g is applied

As discussed earlier in this chapter, when a current pulse is given to the gate the rise and fall times for both V_{ds} and I_{ds} is linear and the rise and fall times can be calculated using equation 5.14.

Parameter	Value
V_{gs}	20 V
$V_{plateau}$	8.3 V
C_{rss1}	310 pF
C_{rss2}	1200 pF
C_{rss3}	11000 pF
V_{ds_1}	1 V
V_{ds_2}	100 V
V_{ds_3}	10 V

Vds rise time and fall time

The Vds fall and rise times is as shown in figures 5.8 and 5.9. The following tables show a calculation of the fall time (t_{fu}) and rise time (t_{ru}).

V_{ds} **Fall Time Calculation**	
Parameter	**Value**
ig	3 A
$\Delta tfu1$	72.33 ns
$\Delta tfu2$	36 ns
$\Delta tfu3$	33 ns
tfu	141.33 ns

V_{ds} **Rise Time Calculation**	
Parameter	**Value**
ig	3 A
$\Delta tru1$	72.33 ns
$\Delta tru2$	36 ns
$\Delta tru3$	33 ns
tru	141.33 ns

Ids Rise time and Fall time

Similarly, the rise time (t_{ri}) and the fall time (t_{fi}) of the drain current (I_d) is as shown in figures 5.10 and 5.11 and calculated as shown in tables below.

The turn on (t_{on}) and turn off (t_{off} times when i_g is applied is calculated as,

I_{ds} **Rise Time Calculation**	
Parameter	**Value**
ig	3 A
C_{iss} at $V_{ds} = 400$V	31.7 nF
C_{rss} at $V_{ds} = 400$V	220 pF
$C_{iss} - C_{rss}$	31.48 nF
V_{pl}	8.3 V
V_{th}	3.2 V
dV	5.1 V
tri	53.52 ns

I_{ds} **Fall Time Calculation**	
Parameter	**Value**
ig	3 A
C_{iss} at $V_{ds} = 400$V	31.7 nF
C_{rss} at $V_{ds} = 400$V	220 pF
$C_{iss} - C_{rss}$	31.48 nF
V_{pl}	8.3 V
V_{th}	3.2 V
dV	5.1 V
tfi	53.52 ns

	Parameter	**Value**
Turn on time	$t_{on} = tfu + tri$	194.85 ns
Turn off time	$t_{off} = tru + tfi$	194.85 ns

Power Loss With Current source driver

Now, the power loss during switching transitions is calculated as shown in table 5.4,

TABLE 5.4: Switching Parameters and Energy Calculations when ig is applied

Parameter	**Value**	**Unit**
Vds	800	V
Id	400	A
Switching frequency (fsw)	10	kHz
E_{on}	$V_{ds}I_{ds}t_{on}$	31.18 mJ
E_{off}	$V_{ds}I_{ds}t_{off}$	31.18 mJ
P_{sw}	$(E_{on} + E_{off}) \cdot fsw$	623.52 W

In one sine cycle of a 50Hz frequency, one switch operating at 10kHz frequency will toggle 100 times for a half cycle. For each instant the instantaneous current will vary. Therefore the turn on and turn off times for each instant will vary. The above calculations are required to be carried out for instantaneous value of the drain-source current I_{ds}.The power loss in switch during each turn ON and turn OFF in one cycle is as shown in figures 5.12 and 5.13, respectively.

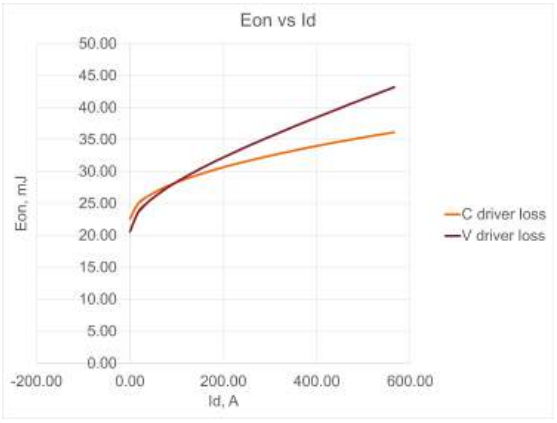

FIGURE 5.12: Switching energy loss during turning ON

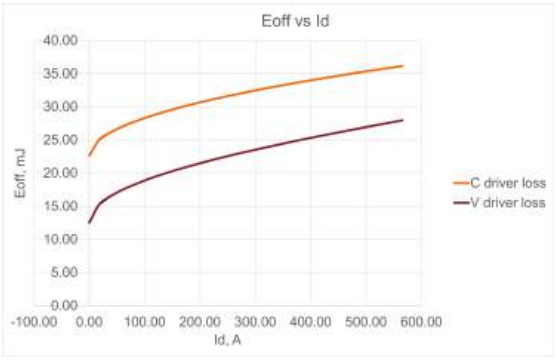

FIGURE 5.13: Switching energy loss during turning OFF

5.3 Conclusion

From tables 5.3 and 5.4, it is evident that the power loss with current 'ig' pulses is lesser than voltage 'vgs' pulses. With higher gate currents the switching times can be reduced further and significantly reduce the power loss.

CHAPTER 6

SIMULATION RESULTS AND ANALYSIS

6.1 Simulation of Double Pulse Test

6.1.1 With Voltage Source Driver

A gate-source voltage (V_{gs}) pulse is applied to the device under test (DUT). The energy loss during switching is observed. The lower MOSFET i.e. Q1 here, serves as the DUT, and the testing conditions are: $V_{gs} = 15\,\text{V}$, switching frequency $f_{sw} = 10\,\text{kHz}$, and a duty cycle of 50%. A simulation has been carried out under these conditions, as illustrated in the following figure 6.1. The results are as shown in 6.2

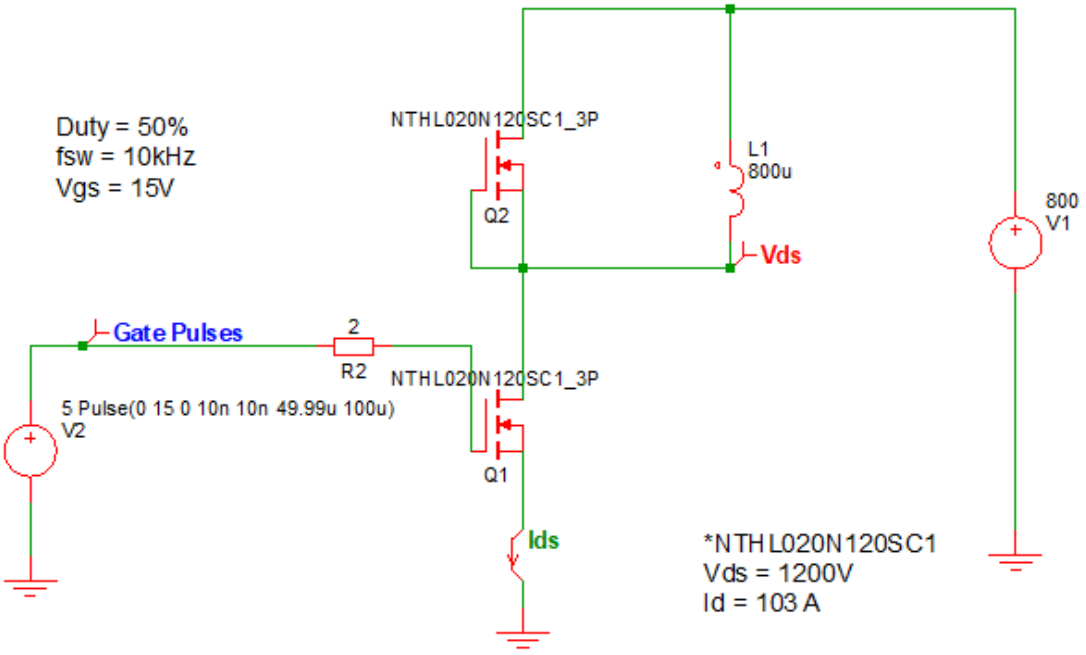

FIGURE 6.1: Simulation model: Double Pulse Test using Voltage Source Driver

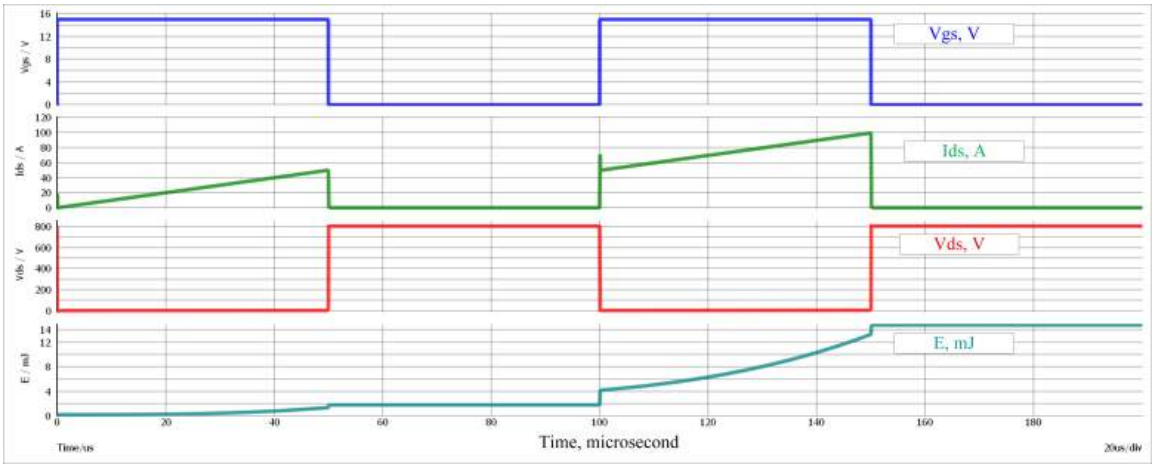

FIGURE 6.2: Results for Voltage Source Double Pulse Test

6.1.2 With Current Source driver

A current pulse is applied to the device under test (DUT). Since the input is a current source, the gate capacitance would continue to charge indefinitely. To prevent this, a diode bridge is connected to limit the gate voltage, as illustrated in Figure 6.3. The lower MOSFET i.e. Q1 here, serves as the DUT. The test is carried out with a gate current $i_g = 10\,\text{A}$, switching frequency $f_{sw} = 10\,\text{kHz}$, and a duty cycle of 50%. The results are as shown in figure 6.4.

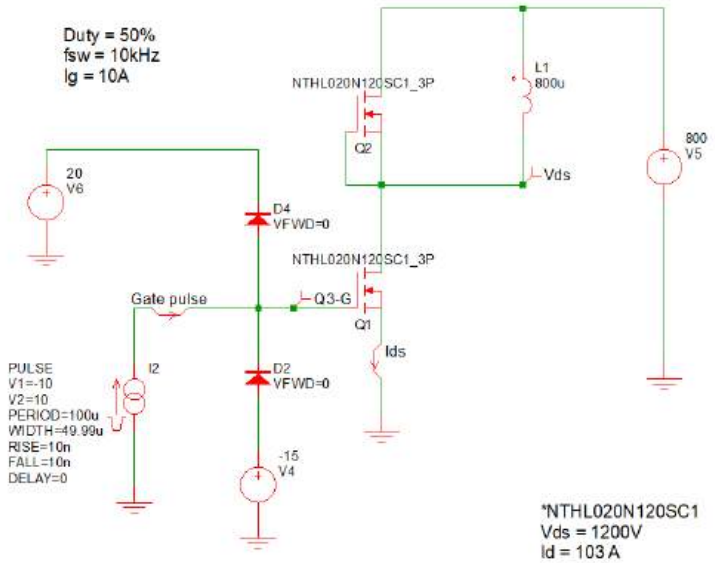

FIGURE 6.3: Simulation model: Double Pulse Test using Current Source Driver

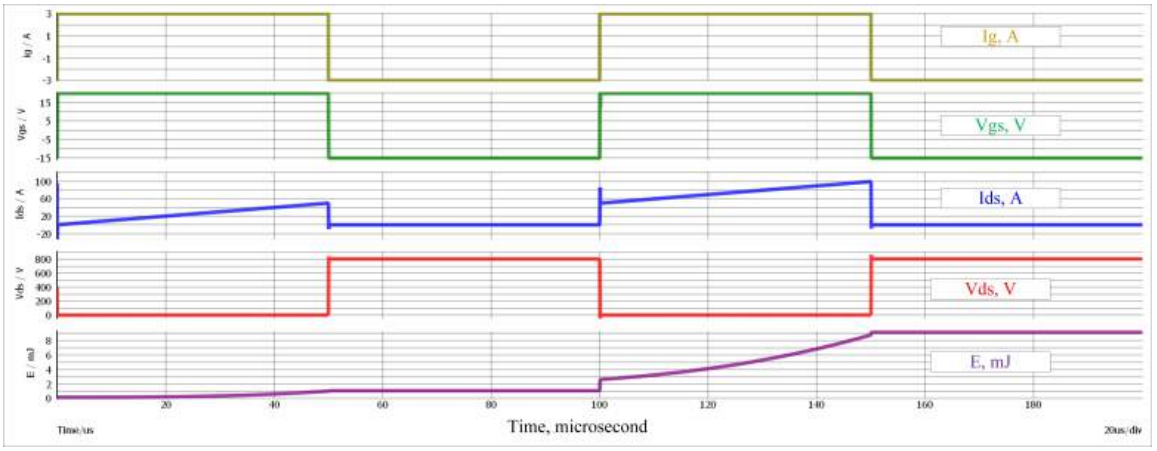

FIGURE 6.4: Results for Current Source Double Pulse Test

6.1.3 Comparison of Switching Energy loss

The switching energy observations made from the above simulation results when current gate pulses i_g and when voltage gate pulses v_{gs} are given are tabulated in the table 6.1 and 6.2, respectively.

Ids	Eon	Eoff
A	mJ	mJ
50	1.54	0.05
100	4.14	0.37
Total switching loss	5.68	0.42

TABLE 6.1: Switching Energy for $I_g = 3A$

Ids	Eon	Eoff
A	mJ	mJ
50	2.4	0.43
100	8.04	1.58
Total switching loss	10.44	2.00

TABLE 6.2: Switching Energy for $V_{gs} = 15V$

The comparison of the turning ON and turning OFF of the switching energy loss in voltage driver and current driver is shown in figures 6.5 and 6.6 respectively.

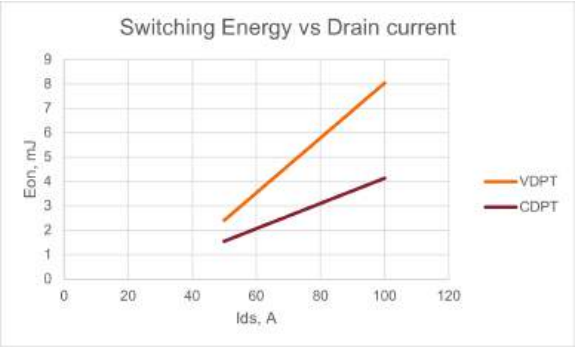

FIGURE 6.5: Switching Energy during turning ON with respect to drain current

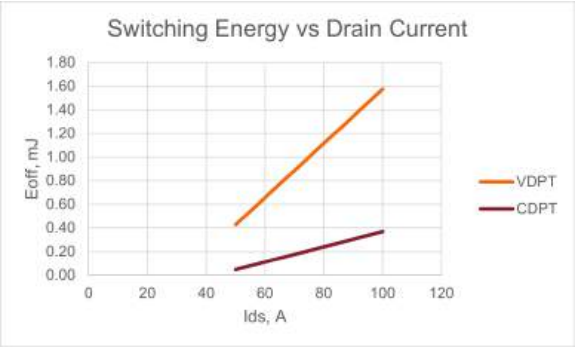

FIGURE 6.6: Switching Energy during turning OFF with respect to drain current

The switching power loss is given by

$$P_{sw} = (E_{on} + E_{off}) * f_{sw} \tag{6.1}$$

Based on a switching frequency (fsw) of 10 kHz and the Eon and Eoff values obtained from the tables, the power loss is calculated to be 124.42 W for the voltage driver and 60.92 W for the current source.

6.2 Simulation of Traction Inverter

Figure 6.7 shows the simulation model of a three phase traction inverter.The inverter is fed with 800 V DC supply.

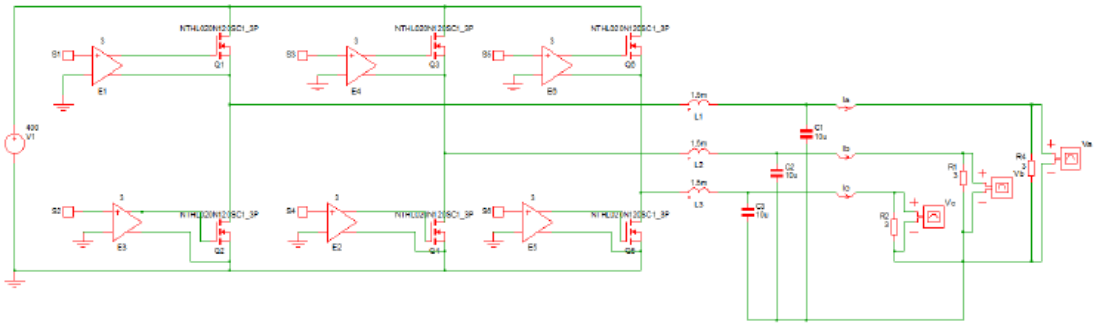

FIGURE 6.7: Simulation model of Three phase inverter

Power loss with Voltage Source

Figure 6.8 shows the output phase voltage and output phase current of the three phase inverter when using Voltage source driver and using Current source driver respectively.

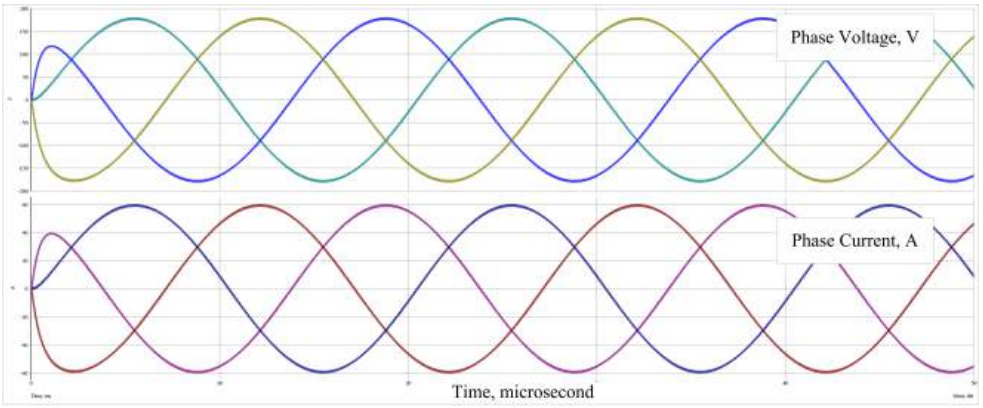

FIGURE 6.8: Inverter Output with Voltage source driver

Figure 6.9 shows the switching energy loss in inverter switches when using a voltage source driver.

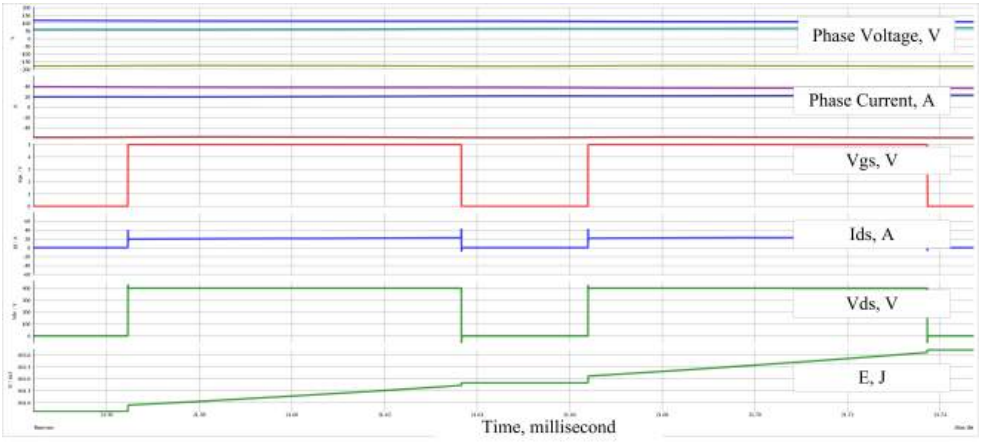

FIGURE 6.9: Energy loss in inverter switch with Voltage Source Driver

Power loss with Current Driver

Figure 6.10 shows the output phase voltage and output phase current of the three phase inverter when using Current source driver.

Figure 6.11 shows the switching energy loss in inverter switches.

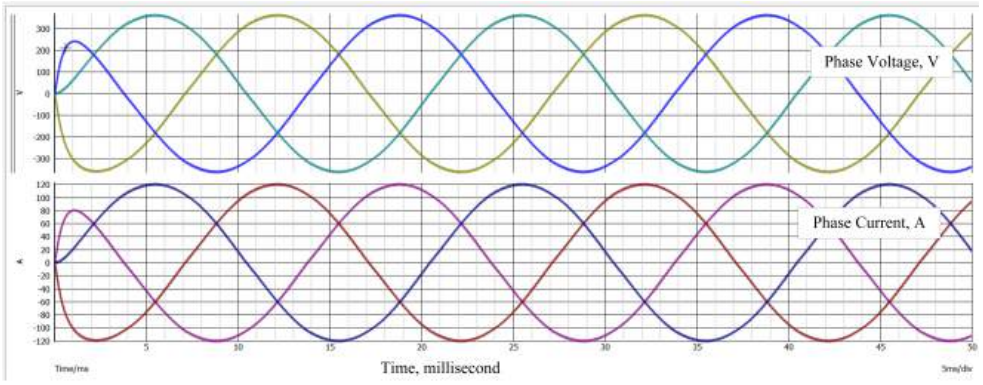

FIGURE 6.10: Inverter Output with Current Source Driver

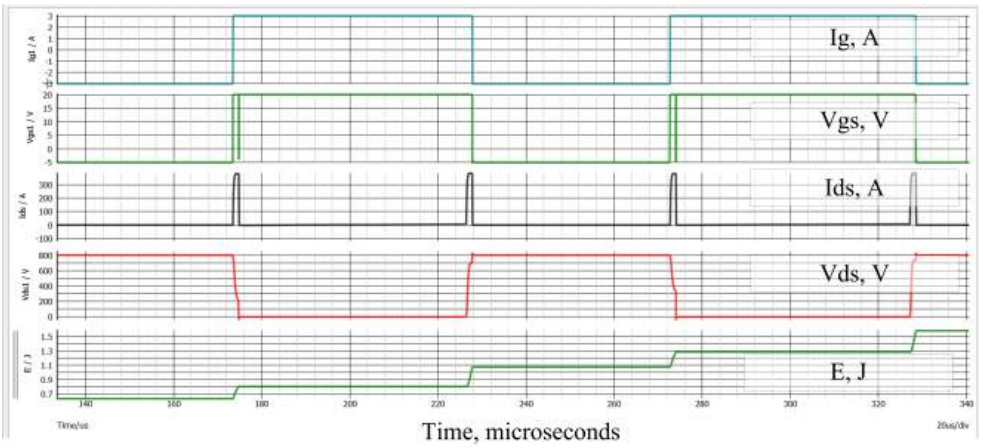

FIGURE 6.11: Energy loss in inverter switch with Current Source Driver

6.3 Hardware Setup of Voltage Source Driver Double Pulse Test

Figure 6.12 shows the evaluation board fed with voltage pulses through a function generator. Figure 6.13 shows the evaluation board. HS and LS are the voltage source gate driver. The device under test is fed with the LS gate driver. The gate-source voltage (V_{gs}), drain-source voltage (V_{ds}) and the inductor current (I_L) re observed, as shown in figure 6.14.

The hardware testing was conducted in a limited setup, making it difficult to verify the results against the simulations. Additionally, the current source gate driver IC is still under development and therefore could not be utilized.

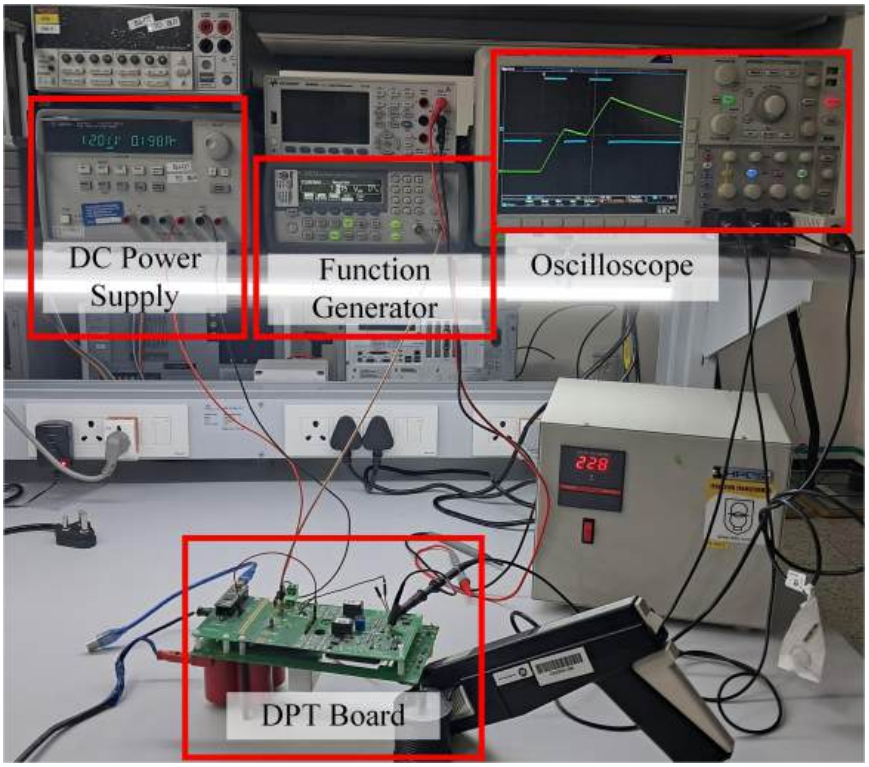

FIGURE 6.12: Hardware Setup of Double Pulse Test with Voltage Source Driver

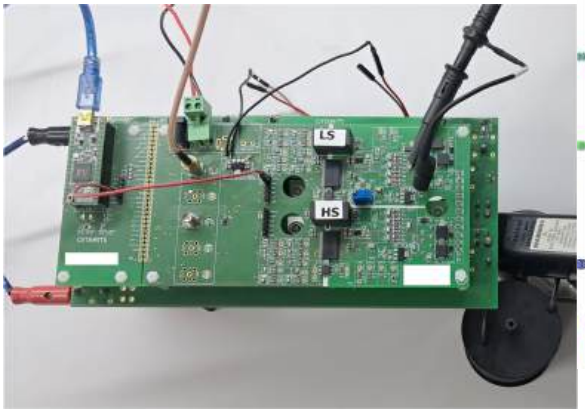

FIGURE 6.13: DPT Evaluation Board

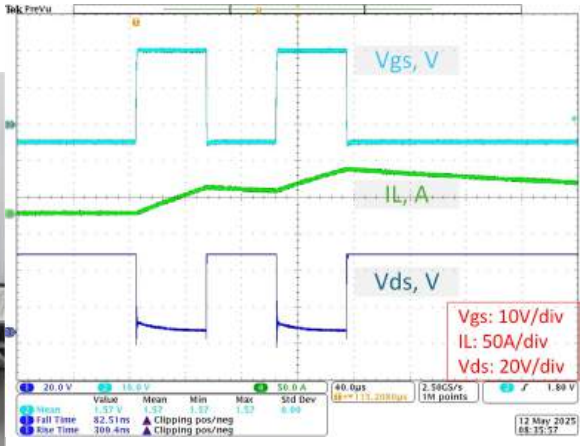

FIGURE 6.14: Waveforms observed on the oscilloscope: gate-source voltage (V_{gs}), drain-source voltage (V_{ds}), and the inductor current (I_L)

CHAPTER 7

CONCLUSION AND FURTHER SCOPE

7.1 Conclusion

With the increase in number of vehicles charging via grid, the power quality of the grid profile is deteriorating. Total Harmonic Distortion (THD) increases with the increase in number of vehicles charging. Based on the various types of grid the THD varies insignificantly.

The performance of a traction inverter is directly related to the performance of the switches which are operated by gate drivers. The current source gate driver is suggested over voltage source gate drivers due to the various advantages it offers. The double pulse test carried out on the MOSFET switches, which suggested that there is using the current source gate driver can reduce the switching losses in the MOSFET which consequently increases the efficiency of the inverter. Due to increased efficiency the driving range of vehicles is increased, which means that the vehicle can travel longer distances in a single charge. This will effectively reduce the charging cycle of the vehicle. This means that the number of times the vehicle to be connected for charging via grid will reduce. This will reduce the injection of harmonics into the grid voltage and current because of the power electronic devices connected in an electric vehicle. Thus, a good quality of power is maintained.

7.2 Future Scope

1. **Analyze the Performance of the Hardware Model of a Current Source Gate Driver Run Traction Inverter**

   This involves examining how the hardware model of a traction inverter, which uses a current source gate driver, performs under various conditions. The goal is to

understand its efficiency, reliability, and overall effectiveness in controlling the electric motor in an electric vehicle (EV).

2. **Study the Impact of EV Charging with Current Source Gate Driver Run Traction Inverter**

   This point focuses on investigating how the use of a current source gate driver in the traction inverter affects the EV charging process. It includes analyzing factors such as charging speed, energy efficiency, and any potential improvements or challenges introduced by this technology.

3. **Analyze Vehicle-to-Grid (V2G) Mode**

   This involves conducting a similar performance analysis for the traction inverter when the EV is operating in Vehicle-to-Grid mode. V2G mode allows the EV to supply power back to the grid, which can help improve power quality and stability. The study would look at how the current source gate driver impacts this process and the benefits it brings to the power grid.

BIBLIOGRAPHY

[1] IEA, "Global ev outlook 2024," 2024. Licence: CC BY 4.0.

[2] Al-Amin, C. Burton, M. Shoeb, S. Ferdous, and G. Shafiullah, "Impact of ev charger on the utility grid and reactive power operation of ev," in *2023 International Conference on Sustainable Technology and Engineering (i-COSTE)*, pp. 1–6, 2023.

[3] L. Pieltain Fernández, T. Gomez San Roman, R. Cossent, C. Mateo Domingo, and P. Frías, "Assessment of the impact of plug-in electric vehicles on distribution networks," *IEEE Transactions on Power Systems*, vol. 26, no. 1, pp. 206–213, 2011.

[4] Y. Yu, D. Reihs, S. Wagh, A. Shekhar, D. Stahleder, G. R. C. Mouli, F. Lehfuss, and P. Bauer, "Data-driven study of low voltage distribution grid behaviour with increasing electric vehicle penetration," *IEEE Access*, vol. 10, pp. 6053–6070, 2022.

[5] S. Gaikwad and H. Mehta, "Investigation of effects of increasing ev penetration on distribution transformers in modi ganpati area, pune," in *2020 IEEE Electric Power and Energy Conference (EPEC)*, pp. 1–5, 2020.

[6] Y. Yu, A. Shekhar, G. C. R. Mouli, P. Bauer, N. Refa, and R. Bernards, "Impact of uncontrolled charging with mass deployment of electric vehicles on low voltage distribution networks," in *2020 IEEE Transportation Electrification Conference & Expo (ITEC)*, pp. 766–772, 2020.

[7] S. Wagh, Y. Yu, A. Shekhar, G. R. C. Mouli, and P. Bauer, "Aggregated impact of ev charger type and ev penetration level in improving pv integration in distribution grids," in *2021 IEEE Transportation Electrification Conference & Expo (ITEC)*, pp. 595–600, 2021.

[8] G. A. Putrus, P. Suwanapingkarl, D. Johnston, E. C. Bentley, and M. Narayana, "Impact of electric vehicles on power distribution networks," in *2009 IEEE Vehicle Power and Propulsion Conference*, pp. 827–831, 2009.

[9] J. Reimers, L. Dorn-Gomba, C. Mak, and A. Emadi, "Automotive traction inverters: Current status and future trends," *IEEE Transactions on Vehicular Technology*, vol. 68, no. 4, pp. 3337–3350, 2019.

[10] H. Gui, Z. Zhang, R. Chen, J. Niu, L. M. Tolbert, F. Wang, B. J. Blalock, D. J. Costinett, and B. B. Choi, "Current source gate drive to reduce switching loss for sic mosfets," in *2019 IEEE Applied Power Electronics Conference and Exposition (APEC)*, pp. 972–978, 2019.

[11] A. Kumar, M. Losito, M. Moradpour, and G. Gatto, "Current source gate driver for sic mosfets in power electronics applications," in *2022 International Symposium on Power Electronics, Electrical Drives, Automation and Motion (SPEEDAM)*, pp. 523–527, 2022.

[12] R. Shahane, S. Belkhode, and A. Shukla, "Current source gate drivers: Topologies, applications, and future research needs," *IEEE Transactions on Power Electronics*, vol. 39, no. 9, pp. 10731–10753, 2024.

[13] H. Gui, Z. Zhang, R. Chen, J. Niu, L. M. Tolbert, F. Wang, D. Costinett, B. J. Blalock, and B. B. Choi, "Gate drive technology evaluation and development to maximize switching speed of sic discrete devices and power modules in hard switching applications," *IEEE Journal of Emerging and Selected Topics in Power Electronics*, vol. 8, no. 4, pp. 4160–4172, 2020.

[14] W. Eberle, Z. Zhang, Y.-F. Liu, and P. C. Sen, "A current source gate driver achieving switching loss savings and gate energy recovery at 1-mhz," *IEEE Transactions on Power Electronics*, vol. 23, no. 2, pp. 678–691, 2008.

[15] L. Balogh, "Fundamentals of mosfet and igbt gate driver circuits," *Texas Instruments–Application report, SLUA618-March*, pp. 28–33, 2017.

[16] J. G. Hayes and G. A. Goodarzi, *Vehicle Dynamics*, pp. 40–67. 2018.